Angewandte Chemie
Eine Zeitschrift der Gesellschaft Deutscher Chemiker

Supporting Information

Molecular Dynamics Simulations Guide Chimeragenesis and Engineered Control of Chemoselectivity in Diketopiperazine Dimerases

V. V. Shende, N. R. Harris, J. N. Sanders, S. A. Newmister, Y. Khatri, M. Movassaghi, K. N. Houk, D. H. Sherman**

Supporting Information

Instrumentation and materials

All UV-Visible spectra were acquired using a single beam Molecular Devices Spectra Max M5 spectrophotometer, with a 1cm quartz cuvette. Analytical HPLC data was acquired using a Shimadzu HPLC system comprised of two LC-20ADXR pumps, a SIL-20ACXR autosampler, and a SPD-M20A diode array detector. Preparatory HPLC was performed using a Beckman Coulter stack comprised of a System Gold 125 solvent module, 168 detector, and SC100 fraction collector. ^{1}H NMR spectra were recorded on Varian 600 MHz spectrometers and are reported relative to residual solvent peak (DMSO-d_6: δ 2.50, CDCl3: δ 7.26). ^{13}C NMR spectra were reported relative to residual solvent peaks (DMSO-d_6: δ 39.50, CDCl3: δ 77). Protected amino acids and peptide coupling reagents were purchased from Combi-Blocks, triethylamine, solvents, and salts were purchased from Millipore Sigma and were all used without additional purification.

Cloning and mutagenesis

The genomic DNA of *Streptomyces* sp. NRRL-S1868 was extracted and purified as prescribed using the Promega Wizard® Genomic DNA Purification Kit. The PCR primers were designed to introduce an NdeI restriction site at the 5′ end of the fragment and a HindIII restriction site 3′ end. The coding sequences were amplified from the genomic DNA of *Streptomyces sp.* NRRL-S1868 using primers for the associated target gene. AspB was cloned into the multi-cloning site of pET28b(+) vector at NdeI and HindIII restriction sites for using Quickchange mutagenesis as previously described.[1] AspB alanine mutants and NzeB chimeras were generated using the single primer Quickchange mutagenesis method. The nucleotide sequences were confirmed by automated sequencing (University of Michigan DNA Sequencing Core).

Expression and purification of cytochromes P450

Plasmids harboring desired P450 were freshly transformed into chemically competent *E. coli* strain C41(DE3) and selected on Luria-Bertani (LB) medium plates containing 50 μg/mL kanamycin. A single colony was grown overnight in 5 mL LB broth containing 50 μg/mL kanamycin, and 1 mL of overnight culture was used to inoculate 500 mL production cultures (2.8 L baffled Fernbach flask) containing 50 μg/mL kanamycin. Production cultures were incubated at 37°C and 160 rpm for approximately 3-4 hours to desired optical density, A_{600nm} = 0.8-1. Protein expression was induced by the addition of 0.8 mM isopropyl β-D-1-thiogalactopyranoside (IPTG) and 1.0 mM δ-5-aminolevulinic acid (w/v) and incubated for 36 h, 28°C at 160 rpm. Cells were harvested by centrifugation at 5000×*g* at 4°C for 10 min and the cell pellet was stored at -80 °C until purification of the protein.

The cell pellet was resuspended in 5% culture volume of lysis buffer (50 mM Tris (pH=7.4), 50 mM NaCl, 2% glycerol, 0.5 mM EDTA, 10 mM β-mercaptoethanol and 1mM phenylmethylsulfonyl fluoride (PMSF) and disrupted by sonication. Cell lysate was centrifugated (50,000 ×*g* for 35 min) and supernatant was filtered (0.4 μM Millipore filter). His6-tagged P450 was purified by affinity chromatography using Ni-NTA (Qiagen) column as previously described[1] and the collected fractions were analyzed by SDS-PAGE. The suitable red fractions were pooled and dialyzed at 4°C three times using 50 mM Tris, pH 7.4 containing 10% glycerol, 50 mM NaCl and 1 mM dithiothreitol (DTT) against a total of 6 L buffer prior to aliquoting and flash freezing in liquid nitrogen for storage at -80 °C.

Analytical scale P450 reaction conditions

Analytical reactions were performed using 10 μM P450, 20 μM Fdx (recombinant, *S. oleracea)* and 6 μM FdR (recombinant, *S. oleracea)*, 3mM of DKP dissolved in DMSO was added, 1 unit of glucose-6-phosphate dehydrogenase (recombinant, *S. cerevisiae)* and a 500 mM glucose-6-phosphate and diluted to a final volume of 250 μL with reaction buffer (50 mM Tris, pH 7.4 containing 10% glycerol, 50 mM NaCl and 1 mM dithiothreitol) and initiated by adding NADPH (1 mM). Two control reactions were performed which included all contents except NADPH or P450. Reactions were incubated at 30 °C for 1 h agitating at 600 rpm in a thermoshaker (Multi-thermoshaker, Benchmark) and quenched via addition 750 μL of methanol, followed by vortexing at full speed

for 30 s. Quenched reactions were centrifuged at 17,000 x gravity to remove insoluble material and supernatant was analyzed by HPLC and resolved using a linear gradient of 5-100% acetonitrile: water (0.1% formic acid) over 30 min (1.5 mL/min flow rate) on a Phenomenex Luna 5µ C-18(2) 100Å, 250 × 4.60mm 5 micron column.

Supplementary Table S1. Primers used in this study.

Purpose	Nucleotide sequence (5'-3')
Cloning AspB into pET28b (forward)	CTGAGAATCTCTACTTCCAAGGCgctagcGTGACCACCACCGCC
Cloning AspB into pET28b (reverse)	ctttcgggctttgttagcagccggatcTCACCAGGTGGCGGG
AspB mutagenic primer (I68A)	GAGGACCCCCGGCTCAGCTCGGAGGCCGCGGCGGCCTCCGGTGC GCCCCGCCAGGAACCG
AspB mutagenic primer (E76A)	TCGGAGGCCGCGATCGCCTCCGGTGCGCCCCGCCAGGCGCCGGT CGAACTCCGGGCGCCC
AspB mutagenic primer (G89A)	CTCCGGGCGCCCGGCACCCGGGCGGACGCGGTCGCGATGCTCCG CGAAGCCGGACTGCGG
AspB mutagenic primer (D88A)	CTCCGGGCGCCCGGCACCCGGGCGGCGGGCGTCGCGATGCTCCG CGAAGCCGGACTGCGG
AspB mutagenic primer (V90A)	CGGGCGCCCGGCACCCGGGCGGACGGCGCGGCGATGCTCCGCG AAGCCGGACTGCGGTCC
AspB mutagenic primer (L175A)	CTCGCCCACTGCGCCGACACCGGGGCGCGGTTCTGCGGAGTCAC GCACGAGGAACAGGTG
AspB mutagenic primer (F177A)	GCCCACTGCGCCGACACCGGGCTGCGGGCGTGCGGAGTCACGCA CGAGGAACAGGTGCAC
AspB mutagenic primer (V239A)	CTCGCCGAGGCCGGCTCGCTCCTCGTCGCGGCCGGCTTCCCGAC CTCGTCGGGATTCCTG
AspB mutagenic primer (A240G)	GCCGAGGCCGGCTCGCTCCTCGTCGTCGGCGGCTTCCCGACCTC GTCGGGATTCCTGTGC
AspB mutagenic primer (T244A)	CTCCTCGTCGTCGCCGGCTTCCCGGCGTCGTCGGGATTCCTGTGC GGCGCGCTGCTCACC
AspB mutagenic primer (L286A)	GTGGAGGAACTCCTGCGGTACACGCCCGCGTCGACCGGCTCGGTC AAGCGGATGGCCACC
AspB mutagenic primer (V291A)	CGGTACACGCCCCTCTCGACCGGCTCGGCGAAGCGGATGGCCAC CGAGGACCTGGAGATC
AspB mutagenic primer (G343A)	CCGGGGCGCGAGGGGCCGATGCACTTCGCGTTCGGCCGGGGCCG CCACTTCTGCCCCGGC
AspB mutagenic primer (F390A)	GCCCCCGAGGAGATCAGCTGGCACGAAGGGCTCGCGTTCCGCCG CCCGCGGGCGATCCCC
AspB mutagenic primer (F391A)	GAGGAGATCAGCTGGCACGAAGGGCTCTTCGCGCGCCGCCCGCG GGCGATCCCCGCC
AspB mutagenic primer (F390A/F391A)	GAGGAGATCAGCTGGCACGAAGGGCTCGCGGCGCGCCGCCCGCG GGCGATCCCC
AspB mutagenic primer (S290A)	CTGCGGTACACGCCCCTCTCGACCGGCGCGGTCAAGCGGATGGC CACCGAGGACCTGG
NzeB mutagenic primer (Q68I)	GTTCAGCTCGGAGGCCGCAATTGCGTCCGGCGCGCCCCGC
NzeB chimeragenesis primer (P43H_V47A)	CGTCTCGGAGGGCACCGGCGACCATCTCTGGCTCGCCACCCGTTA CGCCACCGCCGTC
NzeB chimeragenesis primer (T52A_K55E)	CTCTGGCTCGTGACCCGTTACGCCGCCGCCGTCGAACTCCTGGAG GACTCGCGGTTCAGC
NzeB chimeragenesis primer (S60P_F62L_Q68I)	GCCACCGCCGTCAAGCTCCTGGAGGACCCGCGGCTGAGCTCGGA GGCCGCAATTGCGTCC
NzeB chimeragenesis primer (G87A_A89G_I90V)	GGTCGAGCTGCGGGCGCCCGGCACCCGGGGCGACGCCATCGCGA TGCTCCGCGAGGCCGG
NzeB chimeragenesis primer (Q222H)	CTCAAGCTCATCGCCGAAGCACCCGTCGACCATGGCCCGTTGAGC GACGAGGCGCTCGCC

Supplementary Figure S1. NzeB and AspB sequence alignment.

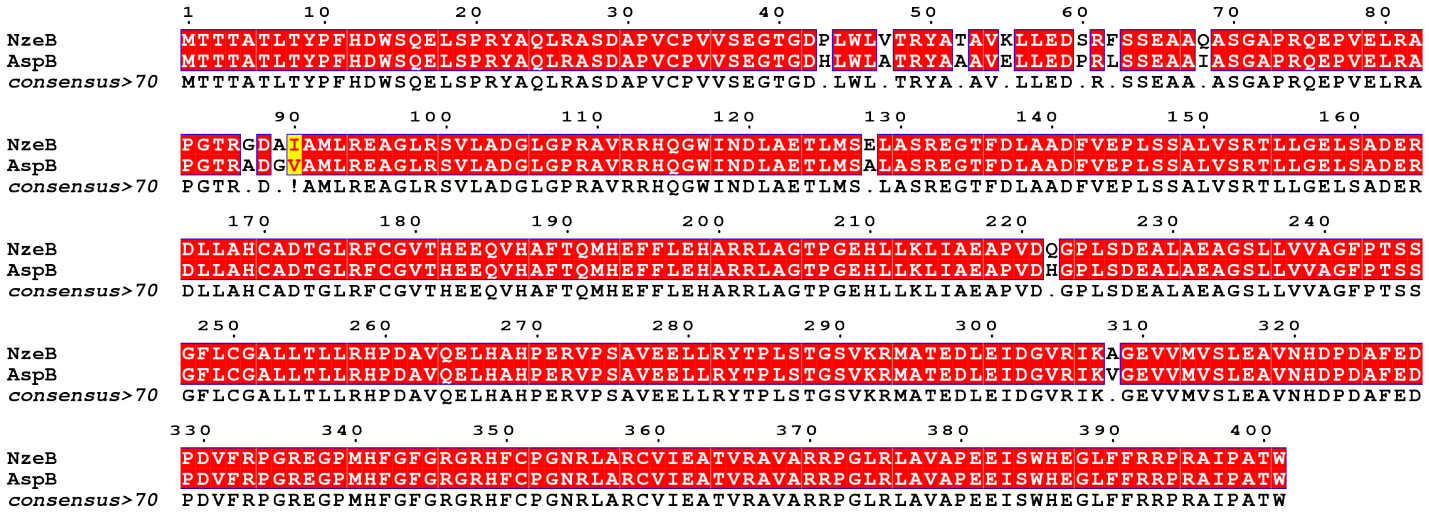

NzeB coding sequence (WP_030888003.1)

VTTTATLTYPFHDWSQELSPRYAQLRASDAPVCPVVSEGTGDPLWLVTRYATAVKLLEDSRFSSEAAQASGA
PRQEPVELRAPGTRGDAIAMLREAGLRSVLADGLGPRAVRRHQGWINDLAETLMSELASREGTFDLAADFVE
PLSSALVSRTLLGELSADERDLLAHCADTGLRFCGVTHEEQVHAFTQMHEFFLEHARRLAGTPGEHLLKLIAEA
PVDQGPLSDEALAEAGSLLVVAGFPTSSGFLCGALLTLLRHPDAVQELHAHPERVPSAVEELLRYTPLSTGSVK
RMATEDLEIDGVRIKAGEVVMVSLEAVNHDPDAFEDPDVFRPGREGPMHFGFGRGRHFCPGNRLARCVIEAT
VRAVARRPGLRLAVAPEEISWHEGLFFRRPRAIPATW

AspB coding sequence (WP_030881046.1)

VTTTATLTYPFHDWSQELSPRYAQLRASDAPVCPVVSEGTGDHLWLATRYAAAVELLEDPRLSSEAAIASGAP
RQEPVELRAPGTRADGVAMLREAGLRSVLADGLGPRAVRRHQGWINDLAETLMSALASREGTFDLAADFVEP
LSSALVSRTLLGELSADERDLLAHCADTGLRFCGVTHEEQVHAFTQMHEFFLEHARRLAGTPGEHLLKLIAEAP
VDHGPLSDEALAEAGSLLVVAGFPTSSGFLCGALLTLLRHPDAVQELHAHPERVPSAVEELLRYTPLSTGSVKR
MATEDLEIDGVRIKVGEVVMVSLEAVNHDPDAFEDPDVFRPGREGPMHFGFGRGRHFCPGNRLARCVIEATV
RAVARRPGLRLAVAPEEISWHEGLFFRRPRAIPATW

Process of crystallization

Crystallization of AspB

Single, diffraction quality crystals of the AspB substrate complex were grown by sitting drop vapor diffusion at 20 °C by mixing 2 µL of 8 mg/mL protein containing 1 mM DKP substrate and 0.2% DMSO with 2 µL of a well solution containing 20% PEG 3350, 300 mM $MgCl_2$, 100 mM Bis-Tris pH 6.5. Sitting droplets were nucleated after 4 h from an earlier spontaneous crystallization using a cat whisker. Single crystals grew after 24 hours. 8 µL of a cryoprotecting solution containing 10 mM Tris pH 7.5, 15 % glycerol, 20% PEG 3350, 300 mM $MgCl_2$, 1 mM DKP substrate, 0.2% DMSO was added directly to the sitting drops and the crystals were harvested using nylon loops and vitrified by rapid plunging into liquid nitrogen. AspB crystallized in space group I2 with unit cell dimensions of a = 68.36 Å, b = 100.62 Å, c = 107.72 Å, α = 90°, β = 92.8°, γ = 90° and two chains in the asymmetric unit.

Data collection and processing

X-ray data were collected at 100 K on beamline 23ID-B at the National Institute for General Medical Sciences (NIGMS) and National Cancer Institute (NCI) Structural Biology Facility at the Advanced Photon Source in Argonne, IL, USA. Diffraction data were integrated and scaled using iMOSFLM[2] and aimless within the CCP4 program suite.[3] Data collection statistics are given in **Supplementary Table S2**.

Molecular replacement, model building and refinement. The structure of AspB was solved by molecular replacement[4] using NzeB (PDB: 6XAJ) as a search model. This resulted in an initial model that could be extended by alternating cycles of manual building in Coot[5] and least-squares refinement with Phenix.[6] Final models were validated using MolProbity.[7]

Crystallization of NzeB chimera (Q68I_ G87A_A89G_I90V)

The purified NzeB quadruple mutant was incubated overnight in 10mM HEPES pH 7.6, 0.2mM DTT, 2% glycerol and supplemented with 1mM of DKP substrate. Crystals were grown by vapor diffusion from 1:1 mixture of 8 mg/mL $NzeB_{Q68IG87AA89GI90V}$ preincubated with substrate and a well solution containing 26% PEG 3350, 2M $MgCl_2$, 100 mM Tris HCl pH 8.5. Sitting droplets were nucleated after 24 h from an earlier spontaneous crystallization using a cat whisker. Single crystals grew after 48 hours. Crystals were cryoprotected in well solution at 15% ethylene glycol and flash-cooled in liquid nitrogen. NzeB crystallized in space group P1 with unit cell dimensions of a = 42.1 Å, b = 92.0 Å, c = 53.9 Å, α = 90°, β = 104°, γ = 90° and two chains in the asymmetric unit.

Data collection and processing

X-ray data were collected at 100 K on beamline 23ID-B at the National Institute for General Medical Sciences (NIGMS) and National Cancer Institute (NCI) Structural Biology Facility at the Advanced Photon Source in Argonne, IL, USA. For $NzeB_{Q68IG87AA89GI90V}$, 360º of diffraction data were collected in inverse-beam geometry using 30º wedges. All data were processed using XDS.[8] The structure was solved by molecular replacement with Phaser-MR[9] using NzeB wild-type (PDB: 6XAJ) as a search model. To generate the initial model, Phenix.autobuild[6] was performed. Iterative rounds of manual building in Coot[5] and refinement with Phenix.refine[6] were used to furnish the final model. Data collection and refinement statistics are given in **Supplementary Table S2**.

Supplementary Table S2. X-ray crystallography data collection statistics.

	AspB in complex with **9** (**PDB:** 7S3J)	$NzeB_{Q68IG87AA89GI90V}$ in complex with **9** (**PDB:** 7S3T)
Wavelength	1.03	1.03
Resolution range	39.76 – 1.94	45.5 - 1.40 (1.45 - 1.40)
Space group	I 2	P 2_1
Unit cell	68.36, 100.62, 107.72 Å 90, 92.76, 90°	42.12, 92.16, 53.94 Å 90, 104.22, 90°
Total reflections	319430 (20371)	462696 (20759)
Unique reflections	53866 (3577)	73441 (4941)
Multiplicity	5.9 (5.7)	6.30 (4.20)
Completeness (%)	99.7 (98.9)	93.8 (63.4)
Mean I/sigma(I)	11.6 (2.0)	17.9 (2.60)
Wilson B-factor	19.5	16.6
R-merge	0.075 (0.916)	0.053 (0.428)
R-meas	0.082 (1.01)	0.058 (0.491)
CC1/2	0.986 (0.347)	0.999 (0.898)
Reflections used in refinement	53674 (5340)	73425 (4940)
R-work	0.226 (0.377)	0.171 (0.265)
R-free	0.292 (0.405)	0.182 (0.309)
Number of non-hydrogen atoms	6514	3534
macromolecules	6094	3073
ligands	186	94
solvent	234	367
Protein residues	800	396
RMS(bonds)	0.008	0.006
RMS(angles)	1.08	0.98
Ramachandran favored (%)	97.72	98.45
Ramachandran allowed (%)	2.16	1.55
Ramachandran outliers (%)	0.13	0.00
Rotamer outliers (%)	1.11	0.00
Average B-factor	25.61	22.38
macromolecules	25.91	21.65
ligands	19.01	18.38
solvent	23.22	29.53

Molecular dynamics methods

Molecular dynamics simulations were prepared and equilibrated using the GPU code (*pmemd*)[10] of the AMBER 16 package.[11] Parameters for the brevianamide F ligands were generated within the *antechamber* module using the general AMBER force field (*gaff*),[12] with partial charges set to fit the electrostatic potential generated at the HF/6-31(d) level by the RESP model.[13] The partial charges were calculated according to the Merz–Singh–Kollman scheme[14,15] using the Gaussian 09 package.[16] Well-established quantum mechanically derived parameters for the heme iron-oxo coenzyme (Compound I) and the covalently-linked cysteine residue were taken from the literature.[17] Each protein was immersed in a pre-equilibrated cubic box with a 10 Å buffer of TIP3P[18] water molecules using the *leap* module, resulting in the addition of around 23,000 solvent molecules. The systems were neutralized by addition of explicit counter ions (Na^+ and Cl^-). All subsequent calculations were done using the widely tested Stony Brook modification of the Amber14 force field (*ff14sb*).[19] Water molecules were treated with the SHAKE algorithm such that the angle between the hydrogen atoms was kept fixed. For the heating and equilibration steps, long-range electrostatic effects were modeled using the particle-mesh-Ewald method.[20] An 8 Å cutoff was applied to Lennard–Jones and electrostatic interactions. First, a geometry optimization was performed on each system to minimize the positions of solvent molecules and ions while imposing positional restraints on the protein backbone and ligands using a harmonic potential with a force constant of 2 kcal·mol^{-1}·Å^{-2}. Second, each system was gently and continuously heated over 1 ns from 0 K to 300 K under constant-volume and periodic-boundary conditions. Harmonic restraints of 2 kcal·mol^{-1} were applied to the protein backbone and ligands, and the Andersen equilibration scheme was used to control and equalize the temperature. The time step was kept at 1 fs during the heating stages, allowing potential inhomogeneities to self-adjust. Third, each system was then equilibrated for a total of 4 ns at constant pressure of 1 atm with a Berendson barostat with a 2 fs time step; harmonic restraints of 2 kcal·mol^{-1} were applied for the first 2 ns and harmonic restraints of 0.5 kcal·mol^{-1} were applied for the second 2 ns to the protein backbone and ligands. Finally, production trajectories without harmonic restraints were run on the Anton 2 supercomputer[21] for 1200 ns with a 2.5 fs time step at 300 K and 1 atm using the default NPT integrator and the default u-series treatment of electrostatic interactions. Three production trajectories were obtained for both the NzeB enzyme and the AspB enzyme.

Supplementary Figure S2. Replicate MD simulations for N–H abstraction.

A. Representation of N–H to iron-oxo distances tracked throughout MD simulation.

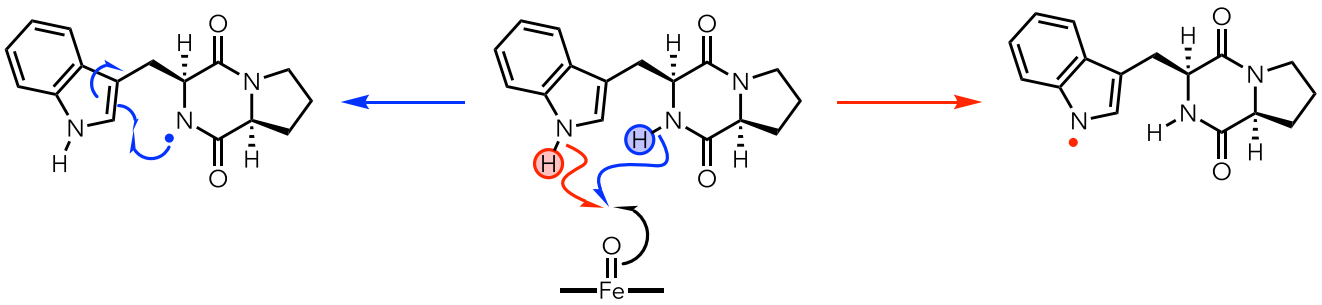

B. MD simulations of NzeB tracking N–H to iron-oxo distances in triplicate.

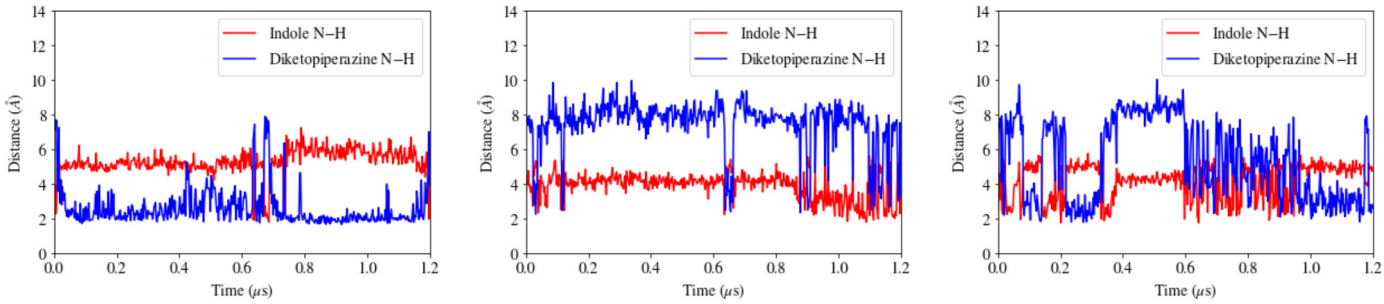

C. MD simulations of AspB tracking N–H to iron-oxo distances in triplicate.

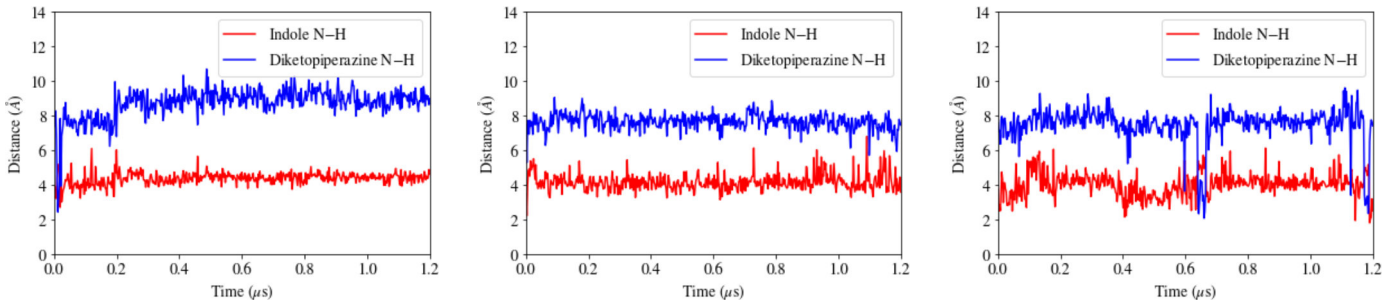

Supplementary Table S3: RMSD for the α-carbon of each amino acid in NzeB and AspB averaged over three 1.2 microsecond MD simulations for each enzyme.

Amino Acid	NzeB RMSD (Å)	AspB RMSD (Å)
6	1.88	1.82
7	0.96	1.09
8	0.91	0.85
9	0.76	0.77
10	0.78	0.83
11	0.84	0.68
12	0.85	0.86
13	0.75	0.91
14	0.74	0.95
15	0.89	0.92
16	0.93	0.89
17	1.46	1.27
18	1.88	1.43
19	2.07	1.97
20	1.22	1.45
21	1.07	1.36
22	1.06	1.57
23	1.22	1.53
24	1.05	1.20
25	0.93	1.16
26	1.03	1.35
27	1.35	1.56
28	1.17	1.58
29	1.38	1.90
30	1.09	1.45
31	1.00	1.28
32	0.74	0.76
33	0.83	0.67
34	0.92	0.76
35	0.81	0.67
36	0.87	0.64
37	0.75	0.63
38	1.45	1.03
39	1.33	1.00
40	0.91	0.73
41	1.00	0.82
42	0.85	0.77
43	0.89	0.75
44	0.72	0.61
45	0.67	0.55
46	0.60	0.53
47	0.67	0.49
48	0.72	0.61
49	0.81	0.69
50	0.75	0.75
51	1.42	0.90
52	0.95	0.66
53	0.84	0.59
54	1.05	0.72
55	1.22	0.79
56	1.02	0.67
57	1.02	0.69
58	1.52	0.93
59	1.47	0.98
60	1.53	1.17
61	1.42	0.85
62	1.29	0.77
63	1.17	0.66
64	1.09	0.68
65	1.39	0.77
66	1.26	1.00
67	1.12	1.07
68	1.64	1.41
69	1.78	1.47
70	2.14	2.03
71	1.96	1.54
72	1.25	0.93
73	0.86	0.63
74	0.76	0.61
75	0.82	0.72
76	0.83	0.78
77	1.33	0.72
78	1.25	0.85
79	1.58	0.97
80	1.41	0.90
81	1.51	0.97
82	1.24	1.08
83	1.36	1.61
84	2.67	2.26
85	2.23	1.77
86	3.82	1.76
87	4.93	1.86
88	4.07	1.83
89	3.49	1.81
90	3.48	2.02
91	3.11	1.98
92	2.41	1.22
93	2.16	2.03
94	2.81	2.26
95	2.73	1.86
96	2.86	1.94
97	3.21	1.66
98	2.65	1.85
99	4.02	3.44
100	1.55	3.40
101	1.23	1.76
102	1.11	1.91
103	1.20	2.73
104	1.15	1.85
105	0.85	0.83
106	0.80	1.00
107	0.90	1.09
108	0.92	0.98
109	1.06	1.30
110	1.00	1.06
111	0.82	0.90
112	1.02	1.18
113	0.98	1.10
114	0.68	0.82
115	0.73	0.80
116	0.74	0.93
117	0.69	0.76
118	0.57	0.64
119	0.65	0.64
120	0.70	0.74
121	0.63	0.71
122	0.64	0.70
123	0.65	0.76
124	0.76	0.81
125	0.63	0.69
126	0.64	0.77
127	0.80	0.88
128	0.93	1.09
129	1.03	1.17
130	1.48	1.80
131	1.65	2.09
132	1.46	1.71
133	1.74	1.98
134	1.67	1.63
135	1.31	1.11
136	1.15	0.97
137	0.99	0.82
138	0.61	0.74
139	0.82	0.73
140	0.89	0.81
141	0.87	0.89
142	0.66	0.66
143	0.74	0.60
144	0.82	0.76
145	0.77	0.82
146	0.77	0.73
147	0.84	0.85
148	0.82	0.91
149	0.75	0.92
150	0.75	0.95
151	0.72	0.93
152	0.73	0.79
153	0.75	0.68
154	0.65	0.68
155	0.60	0.68
156	0.66	0.84
157	0.91	0.88
158	0.91	1.05
159	1.21	1.24
160	1.15	1.13
161	1.49	1.23
162	1.30	0.99
163	1.01	0.81
164	0.89	0.86
165	0.95	0.88
166	0.92	0.77
167	0.75	0.72

168	0.73	0.82
169	0.87	0.66
170	0.76	0.58
171	0.83	0.61
172	0.82	0.69
173	0.85	0.70
174	0.75	0.51
175	0.69	0.45
176	0.68	0.58
177	1.09	0.66
178	1.24	0.86
179	1.31	1.12
180	1.14	1.06
181	1.29	1.10
182	1.23	1.28
183	1.24	1.33
184	1.23	1.29
185	1.01	0.97
186	0.99	0.86
187	0.87	0.89
188	0.85	0.71
189	0.85	0.65
190	0.95	0.71
191	0.92	0.71
192	0.94	0.73
193	1.11	0.68
194	1.20	0.68
195	1.00	0.68
196	0.91	0.74
197	1.09	0.82
198	1.33	0.86
199	0.88	0.78
200	0.86	0.90
201	1.04	1.05
202	0.94	0.90
203	0.83	0.89
204	1.03	0.98
205	1.16	1.16
206	1.17	1.22
207	1.38	1.31
208	1.24	1.06
209	1.06	1.04
210	0.73	0.82
211	0.74	0.76
212	0.62	0.67
213	0.74	0.73
214	0.98	0.78
215	0.95	0.84
216	0.98	0.96
217	1.43	1.41
218	1.82	1.53
219	2.51	2.79
220	2.57	2.79
221	2.61	3.82
222	2.69	3.59
223	2.44	2.68
224	2.34	2.05
225	1.56	1.27
226	1.89	1.20
227	1.73	1.06
228	2.17	0.96
229	2.04	1.04
230	1.47	1.03
231	1.39	0.86
232	1.49	0.86
233	1.40	0.91
234	1.07	1.01
235	1.31	0.79
236	1.35	0.62
237	1.04	0.73
238	0.95	0.76
239	1.11	0.88
240	1.22	0.91
241	0.88	1.32
242	1.18	1.07
243	0.96	0.86
244	0.76	0.64
245	0.86	0.74
246	0.78	0.70
247	0.75	0.57
248	0.66	0.67
249	0.69	0.67
250	0.66	0.61
251	0.73	0.76
252	0.77	0.71
253	0.86	0.81
254	0.76	0.77
255	0.76	0.77
256	0.95	0.86
257	1.05	0.92
258	1.17	0.99
259	1.50	1.17
260	2.35	1.77
261	2.67	1.53
262	2.28	1.33
263	1.83	0.97
264	1.99	1.11
265	2.23	1.17
266	2.09	1.00
267	2.46	1.27
268	2.59	1.49
269	2.02	1.50
270	1.90	1.29
271	1.96	1.36
272	1.22	1.13
273	0.81	0.82
274	0.94	0.89
275	0.91	0.90
276	0.67	0.73
277	0.66	0.64
278	0.55	0.74
279	0.49	0.58
280	0.61	0.55
281	0.64	0.60
282	0.48	0.56
283	0.53	0.54
284	0.54	0.52
285	0.64	0.51
286	0.56	0.58
287	0.53	0.58
288	0.79	0.54
289	0.72	0.58
290	0.58	0.49
291	0.65	0.58
292	0.71	0.53
293	0.76	0.51
294	0.92	0.63
295	1.10	0.73
296	1.21	0.85
297	1.41	1.02
298	1.55	1.22
299	1.46	1.27
300	1.82	1.25
301	1.76	1.26
302	2.06	1.58
303	2.66	1.98
304	2.20	1.37
305	2.03	1.24
306	1.56	1.12
307	1.57	1.01
308	1.51	0.87
309	1.38	0.81
310	1.12	0.79
311	0.78	0.66
312	0.67	0.56
313	0.57	0.60
314	0.54	0.46
315	0.51	0.49
316	0.65	0.57
317	0.76	0.52
318	0.68	0.52
319	0.55	0.47
320	0.53	0.64
321	0.72	0.95
322	0.77	0.74
323	0.90	0.88
324	1.08	0.92
325	1.00	0.96
326	0.91	0.90

327	1.03	1.00
328	1.15	1.18
329	0.98	1.08
330	1.23	1.02
331	1.26	1.02
332	1.10	1.03
333	1.14	1.09
334	1.23	1.75
335	1.75	2.65
336	1.54	1.80
337	2.23	2.44
338	2.68	2.28
339	1.35	1.14
340	1.44	1.18
341	0.86	0.84
342	0.83	1.06
343	1.07	0.90
344	0.97	0.68
345	1.15	0.91
346	1.21	1.10
347	1.55	1.35
348	1.50	1.27
349	0.83	0.74
350	0.83	0.74
351	0.71	0.60
352	0.85	0.83
353	0.68	0.78
354	0.56	0.74
355	0.67	0.81
356	0.75	0.71
357	0.70	0.69
358	0.65	0.71
359	0.61	0.72
360	0.69	0.64
361	0.91	0.77
362	0.60	0.79
363	0.63	0.74
364	0.79	0.76
365	0.86	0.79
366	0.75	0.82
367	0.84	0.78
368	0.92	0.85
369	0.98	0.85
370	1.18	0.98
371	1.19	1.01
372	1.35	1.12
373	1.54	1.41
374	0.95	1.27
375	1.08	1.13
376	0.94	1.10
377	1.05	1.20
378	1.46	1.17
379	1.59	1.24
380	1.23	1.17
381	1.49	1.54
382	1.26	1.25
383	0.67	0.83
384	0.82	0.89
385	0.59	0.79
386	0.68	0.62
387	1.07	0.87
388	0.83	0.85
389	0.67	0.60
390	0.67	0.59
391	0.55	0.58
392	0.75	0.56
393	0.64	0.49
394	0.59	0.56
395	0.74	0.77
396	0.73	0.74
397	0.68	0.65
398	0.96	0.79
399	0.83	0.89
400	1.09	0.87
401	1.09	1.32

Supplementary Figure S3. Dimerization reactions of AspB alanine mutants.

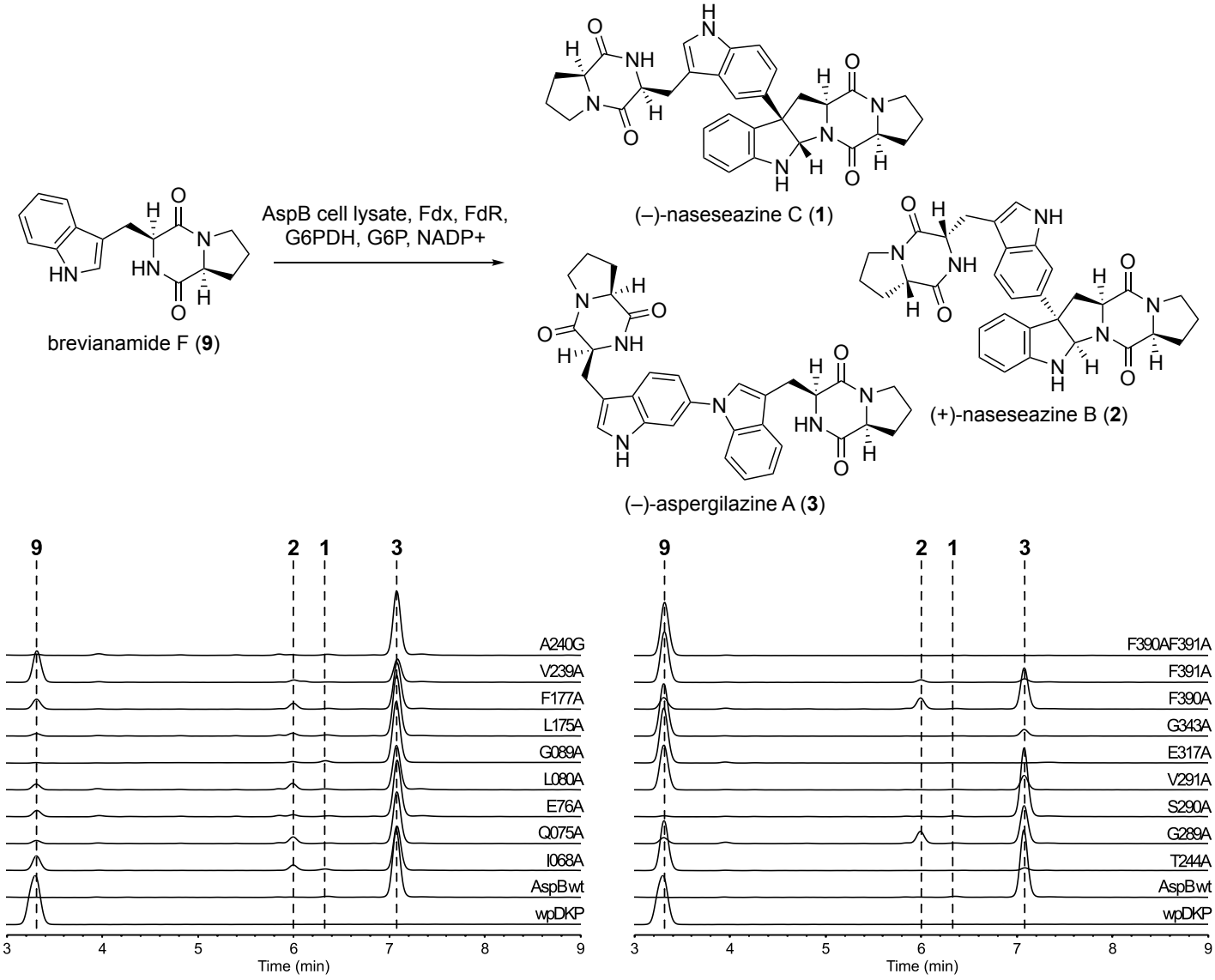

AspB mutants were expressed in 50 mL cultures and the resulting cell pellet was suspended in 5mL of buffer (HEPES 50 mM, pH=7.5, 300 mM NaCl ,10% glycerol, 0.75 mg/mL lysozyme, and 1 mM PMSF). Sonication was performed for one minute total working time and 250 µL of DNase (2 mg/mL) added post-sonication. Cell lysate was centrifuged at 50,000 × g for 15 minutes and supernatant was collected for determination of active P450 concentration. Lysate reactions were performed at a final volume of 250 µL volumes, final active P450 concentration (5 µM), with electron donors from *S. oleracea:* (20 uM Fdx, 6 uM FdR), and a recycling system containing 100 mM G6P, 1 unit/mL G6PDH, and 1 mM NADP+. Reactions including all the contents except for NADPH or P450 were used as controls. The reaction was incubated at 30°C for 1 h agitating at 600 rpm in a thermoshaker (Multi-thermoshaker, Benchmark) and quenched through addition of an equal volume of chloroform and the biphasic solution was extracted with chloroform 3 times. The samples were dried under a stream of nitrogen and the residue was resuspended in 100 µL of HPLC grade methanol and analyzed by HPLC in which the reaction mixture was resolved using a linear gradient of 5-100% acetonitrile:water (0.1% formic acid) over 30 min (1.5 mL/min flow rate) on a Phenomenex Luna 5µ C-18(2) 100Å, 250 × 4.60mm 5 micron column.

Supplementary Figure S4. Synthesis of substrate mimic **10**.

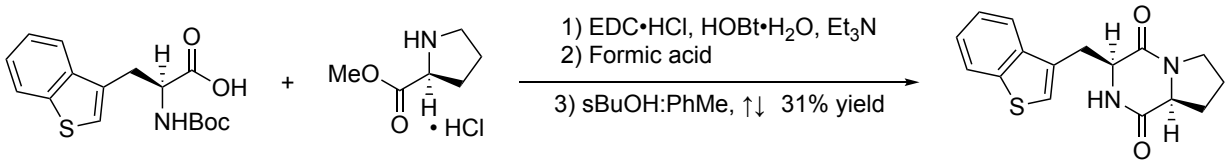

10

To a 250 mL round bottom flask was added *L*-proline methyl ester hydrochloride (5.0 g, 30.2 mmol, 1.05 equiv.) which was dissolved in anhydrous DMF (75 mL, 0.4 M) under an inert atmosphere of N_2. To this solution was added triethylamine (4.2 mL, 30.2 mmol, 1.0 equiv.) which formed a precipitate, and this mixture was allowed to stir at room temperature for 20 minutes. After 20 minutes, Boc-3-(3-benzotheinyl)-*L*-alanine (9.2 g, 28.7 mmol, 1.0 equiv.), EDC·HCl (5.5 g, 28.7 mmol, 1.0 equiv.), and HOBt·H_2O (4.5 g, 28.7 mmol, 1.0 equiv.), were added in quick succession, the headspace of the reaction was purged with N_2 and the reaction was allowed to proceed for 12 hours at which point the reaction had reached completion by TLC. The reaction was quenched by addition of 1 volume each of 1 M HCl and distilled H_2O and was extracted with EtOAc (3 × 100 mL). EtOAc fractions were washed with $NaHCO_3$ to remove excess unreacted carboxylic acid, then washed exhaustively with a 1 M LiCl solution to remove DMF (as indicated by TLC), dried over $MgSO_4$, filtered, and solvent was removed in vacuo to give a soft foam which was used directly with no additional purification.

To the resulting bis-protected dipeptide was added neat formic acid (40 mL) and the mixture was allowed to stir for 4 hours when full Boc-deprotection was indicated by TLC. Formic acid was removed in vacuo to give a thick, yellow oil which was immediately dissolved in a 4:1 solution of *s*BuOH:Toluene (75 mL, 0.4 M) and heated to reflux for 12 hours. To aid in precipitation of diketopiperazine product upon cooling, hexanes was added and the flask was stored at 4 ºC until cool. Solid was collected by filtration and triturated with hot acetone to give diketopiperazine **10** as an off-white powder (2.7 g, 31% yield overall).

HRMS (ESI-TOF): m/z $[M+H]^+$ calculated for $C_{16}H_{17}N_2O_2S^+$ = 301.1005, observed = 301.1035 $[M+H]^+$, 323.0833 $[M+Na]^+$.

^{1}H NMR (599 MHz, $CDCl_3$) δ 7.91 – 7.86 (m, 1H), 7.78 – 7.73 (m, 1H), 7.44 – 7.36 (m, 2H), 7.28 (s, 1H), 4.46 – 4.35 (m, 1H), 4.07 (t, J = 8.0 Hz, 1H), 3.87 (dd, J = 15.2, 3.4 Hz, 1H), 3.71 – 3.55 (m, 2H), 3.06 (dd, J = 15.2, 11.0 Hz, 1H), 2.33 (dt, J = 11.7, 6.8 Hz, 1H), 2.04 (q, J = 8.3 Hz, 2H), 1.91 (ddd, J = 15.8, 10.2, 7.2 Hz, 1H).

^{13}C NMR (151 MHz, $CDCl_3$) δ 169.29, 164.95, 140.89, 137.94, 130.64, 124.92, 124.53, 124.48, 123.26, 121.35, 59.18, 54.06, 45.53, 29.94, 28.29, 22.60.

Supplementary Figure S5. Synthesis and purification of oxidized products **11/11'**.

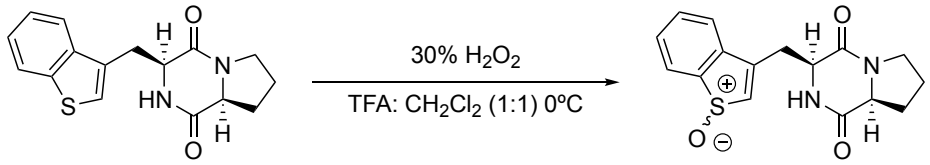

10 **11/11'**

Reactions were performed using conditions from a recently reported synthetic procedure for oxidation of substituted benzothiophenes to their corresponding benzothiophene sulfoxides.[22] Diketopiperazine **10** (100 mg, 0.333 mmol, 1.0 equiv.) was dissolved in a premixed 1:1 solution of TFA:CH_2Cl_2 (0.05 M) chilled to 0 ºC. Once fully dissolved H_2O_2 (30 % in H_2O, 100 uL, 0.33 mmol, 1.1 equiv.) was added in a single addition and reaction was allowed to stir until all starting material was consumed by HPLC-MS. Note: if additional equivalents of H_2O_2 are used, reaction is allowed to proceed for longer reaction times, or allowed to warm to r.t., significant quantities of sulfone begin to form. Solvent was removed in vacuo and residue was resuspended in MeOH, filtered and purified via preparatory HPLC (Luna preparative HPLC column, C18, 5 µm, 21.2 × 250 mm) using gradient of 10% to 50% acetonitrile : water (0.1% formic acid) over 45 min with a flowrate of 4.0 mL/min. Product **11/11'** eluted as two peaks of identical mass and fragmentation pattern (**11'** t_R = 14.327 min, **11** t_R = 14.947 min), presumed to be diastereomeric at sulfur. Fractions eluting later were pooled and demonstrated to co-elute with enzymatic product, and the mixed fractions was subjected to two additional rounds of purification to yield pure product (**11'** = 11.4 mg, 0.034 mmol, 11 % yield, **11** = 10.3 mg, 0.032 mmol, 10 % yield).

Early eluting fraction (**11'**):

HRMS (ESI-TOF): m/z $[M+H]^+$ calculated for $C_{16}H_{17}N_2O_2S^+$ = 317.0954, observed = 317.0961$[M+H]^+$.

^{1}H NMR (599 MHz, $CDCl_3$) δ 7.93 – 7.87 (m, 1H), 7.60 – 7.45 (m, 3H), 6.97 (s, 1H), 6.82 (s, 1H), 4.42 (d, J = 9.1 Hz, 1H), 4.12 (d, J = 8.4 Hz, 1H), 3.71 – 3.52 (m, 3H), 2.95 (dd, J = 16.4, 9.5 Hz, 1H), 2.38 – 2.27 (m, 1H), 2.05 (q, J = 9.6 Hz, 2H), 1.96 – 1.84 (m, 1H).

^{13}C NMR (151 MHz, $CDCl_3$) δ 169.85, 164.18, 145.67, 144.15, 137.21, 133.58, 132.12, 129.37, 126.43, 122.74, 59.23, 53.25, 45.68, 29.32, 28.13, 22.60.

Late Eluting Fraction **(11)**

HRMS (ESI-TOF): m/z $[M+H]^+$ calculated for $C_{16}H_{17}N_2O_2S^+$ = 317.0954, observed = 317.0975 $[M+H]^+$.

^{1}H NMR (599 MHz, $CDCl_3$) δ 7.96 – 7.90 (m, 1H), 7.59 (dd, J = 8.7, 6.2 Hz, 1H), 7.54 (d, J = 7.3 Hz, 2H), 7.01 (s, 1H), 6.57 (s, 1H), 4.43 (d, J = 10.0 Hz, 1H), 4.13 (t, J = 7.9 Hz, 1H), 3.69 – 3.53 (m, 3H), 2.90 (dd, J = 16.6, 10.2 Hz, 1H), 2.27 (tdd, J = 12.1, 8.5, 4.2 Hz, 1H), 2.12 – 1.98 (m, 2H), 1.91 (qd, J = 9.3, 3.2 Hz, 1H).

^{13}C NMR (151 MHz, $CDCl_3$) δ 169.98, 164.35, 145.92, 144.80, 137.42, 133.53, 132.21, 129.46, 126.43, 122.63, 59.21, 53.13, 45.68, 29.41, 28.00, 22.71.

Supplementary Figure S6. Synthesis of substrate mimic **S1**.

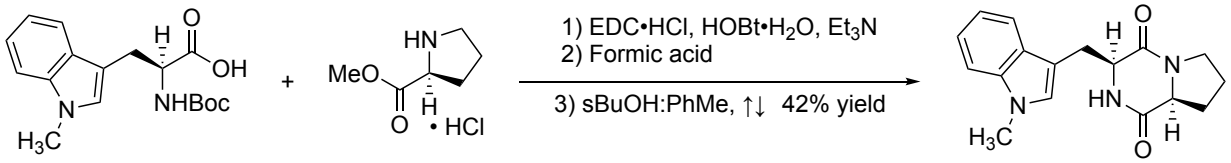

S1

S1 was synthesized using identical conditions as those for substrate mimic **10** (2.3 g 43% yield).

HRMS (ESI-TOF): m/z $[M+H]^+$ calculated for $C_{16}H_{17}N_2O_2S^+$ = 301.1005, observed = 301.1035 $[M+H]^+$, 323.0833 $[M+Na]^+$.

^{1}H NMR (599 MHz, DMSO-d_6) δ 7.59 (dt, J = 8.0, 1.0 Hz, 1H), 7.37 (dt, J = 8.2, 0.9 Hz, 1H), 7.16 – 7.11 (m, 2H), 7.01 (ddd, J = 7.9, 7.0, 1.0 Hz, 1H), 4.30 (t, J = 5.4 Hz, 1H), 4.11 – 4.05 (m, 1H), 3.73 (s, 3H), 3.41 (dt, J = 11.6, 8.0 Hz, 1H), 3.31 – 3.22 (m, 2H), 3.06 (dd, J = 14.9, 5.8 Hz, 1H), 2.00 (dtd, J = 12.2, 6.9, 3.0 Hz, 1H), 1.77 – 1.61 (m, 2H), 1.43 (dtd, J = 12.2, 10.2, 7.8 Hz, 1H).

^{13}C NMR (151 MHz, DMSO-d_6) δ 169.10, 165.49, 136.40, 128.71, 127.71, 121.01, 118.87, 118.34, 109.42, 108.71, 58.44, 55.23, 44.61, 32.29, 27.68, 25.58, 21.93.

Supplementary Figure S7. Synthesis of substrate mimic **S2**.

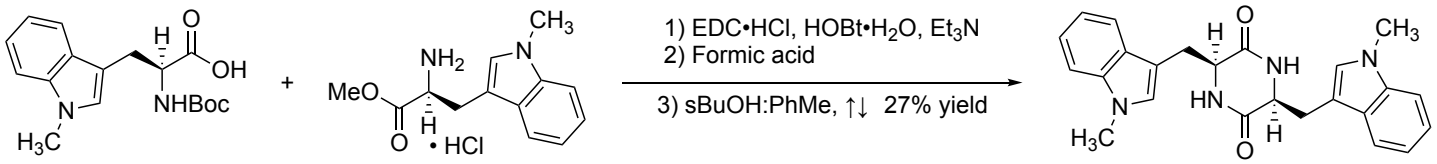

S2

S2 was synthesized using identical conditions as those for substrate mimic **10** (1.9 g 27% yield).

HRMS (ESI-TOF): m/z $[M+H]^+$ calculated for $C_{16}H_{17}N_2O_2S^+$ = 301.1005, observed = 301.1035 $[M+H]^+$, 323.0833 $[M+Na]^+$.

^{1}H NMR (599 MHz, DMSO-d_6) δ 7.76 (d, J = 2.7 Hz, 2H), 7.35 (ddt, J = 14.4, 8.2, 0.9 Hz, 4H), 7.13 (ddd, J = 8.1, 7.0, 1.1 Hz, 2H), 7.01 (ddd, J = 8.0, 7.0, 1.0 Hz, 2H), 6.55 (s, 2H), 3.86 (dt, J = 6.8, 3.5 Hz, 2H), 3.66 (s, 6H), 2.69 (dd, J = 14.3, 4.2 Hz, 2H), 2.17 (dd, J = 14.3, 6.7 Hz, 2H)

^{13}C NMR (151 MHz, DMSO-d_6) δ 166.61, 136.50, 128.73, 127.75, 120.96, 118.82, 118.50, 109.48, 108.11, 55.28, 32.25, 29.81.

Supplementary Figure S8. Analytical and preparatory scale reaction of **10** with NzeB**.**

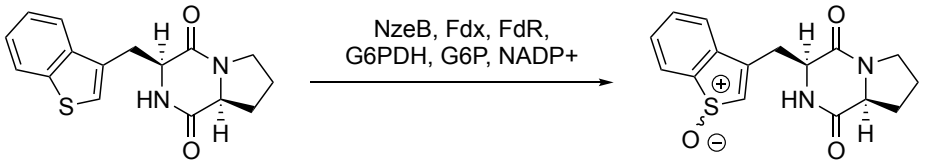

10 **11**

Preparatory Scale

NzeB was expressed as previously reported,[1] and conversion of **10** by NzeB was performed under identical conditions as those used for analytical scale reactions with 2mM of benzothiophene DKP **10** and a final volume of 20 mL. The reaction was quenched via addition of 60 mL of HPLC-grade methanol, split between two 50 mL conical tubes and vortexed on the highest setting for 1 minute. This mixture was then passed through a pad of Celite© and the filter cake was washed with an additional 20 mL of methanol. Methanol was removed in vacuo and aqueous material was extracted 3x with 50 mL of chloroform. Organic layers were dried over $MgSO_4$, filtered and solvent was removed in vacuo. The resulting residue was resuspended in HPLC grade methanol with sonication, insoluble particulates were removed via filtration (0.2 µm syringe filter) and the filtered solution was then purified via preparative HPLC (Luna preparative HPLC column, C18, 5 µm, 21.2 × 250 mm;) using gradient of 5% to 100% acetonitrile : water (0.1% formic acid) over 45 min with a flowrate of 4.0 mL/min. Product **11** eluted at t_R = 5 min and residual starting material **10** t_R = 18 min, and product-containing fractions were pooled, solvent was removed in vacuo, to give < 1 mg of the hydroxylated benzothiophene product **11** which was used for detailed NMR characterization without any further purification.

Analytical Scale

Analytical reaction with substrate mimic **10** and NzeB was performed under identical conditions as those used for analytical scale reactions mentioned previously. Chromatographic conditions were identical to analytical reactions and were performed using an Agilent 6545 LC/QTOF system operating in positive mode, monitoring a mass range of 200 to 1200 amu with ESI-MS, and UV (195−400 nm) detection. ESI conditions were set with the capillary temperature at 320 °C, source voltage at 3.5 kV, and a sheath gas flow rate of 11 L/min and the first 1 min of flow was diverted to waste.

Supplementary Figure S9. Mechanistic proposal for observed sulfoxidation reaction by NzeB.

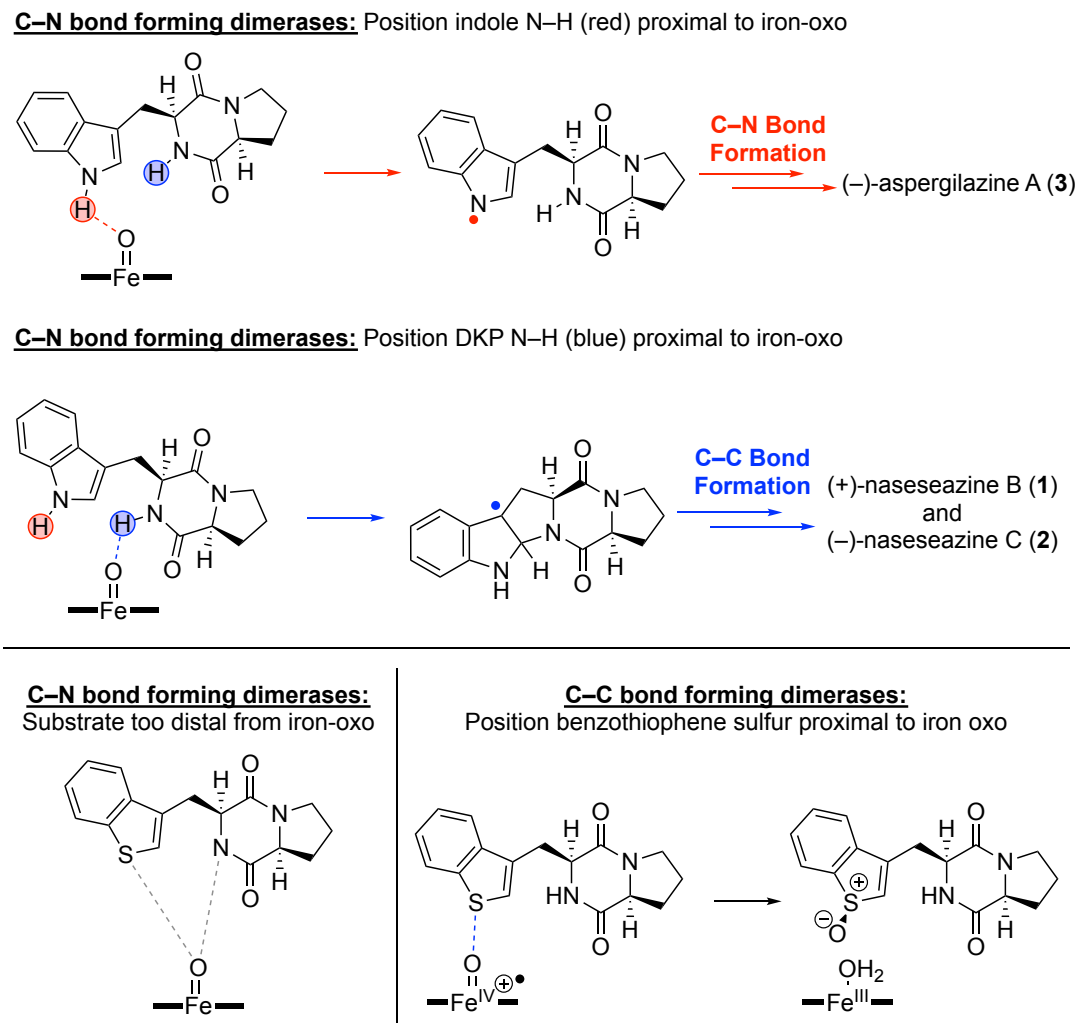

The basis for selectivity in dimerization uncovered by our MD simulations suggests that positioning of substrate in the active site of a given dimerase determines the outcome with dimerization, with C–N bond forming dimerases positioning the indole N–H proximal to the iron-oxo and C–C bond forming dimerases positioning the DKP N–H proximal to the iron-oxo. We hypothesize that the increased size of the benzothiophene heterocycle in **10** compared to indole in substrate in **9** causes **10** to bind in an alternative pose relative to **9** in the enzyme active sites. While at first glance, the sulfoxidation of **10** does appear to be more "C–N bond forming-like" given that there is no N–H to be abstracted we propose this alternative binding mode of **10** causes a change in overall oxidation mechanism wherein C–C bond forming P450s oxidize the benzothiophene via direct oxo-transfer or single-electron oxidation followed by rebound oxygenation,[23] and that only the C–C bond forming P450s position **10** for such reactivity to occur. We note that the intent of this experiment to demonstrate that C–C and C–N bond forming dimerases position substrates differentially, and not to determine/validate an electron or H-atom transfer mechanism of these P450s, which have already been explored computationally. Moreover, product **11** is formed as a single stereoisomer, indicating that this reaction occurs in the enzyme active site, and is not resulting through formation of diffusible hydrogen peroxide or other oxidants. We also discount a change in oxidant, such as iron hydroperoxo, as model complexes have demonstrate these species to be "sluggish" oxidants for sulfoxidation.[24]

Supplementary Figure S10. Analytical reactions of **S1** and **S2** with NzeB and AspB**.**

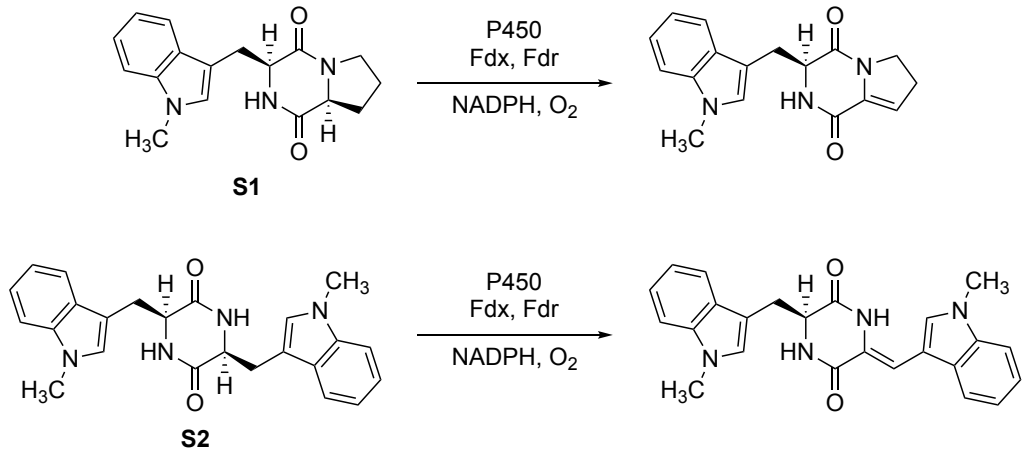

Analytical reaction with substrate mimics **S1** and **S2** with NzeB and AspB was performed under identical conditions as those used for analytical scale reactions mentioned previously. For reactions of both **S1** and **S2** no differential reactivity was observed across all enzymes tested, and by mass spectrometry observed projects corresponded to dehydrogenation.

Supplementary Figure S11. LC-MS spectra (254 nm) for chemical oxidation of **10**.

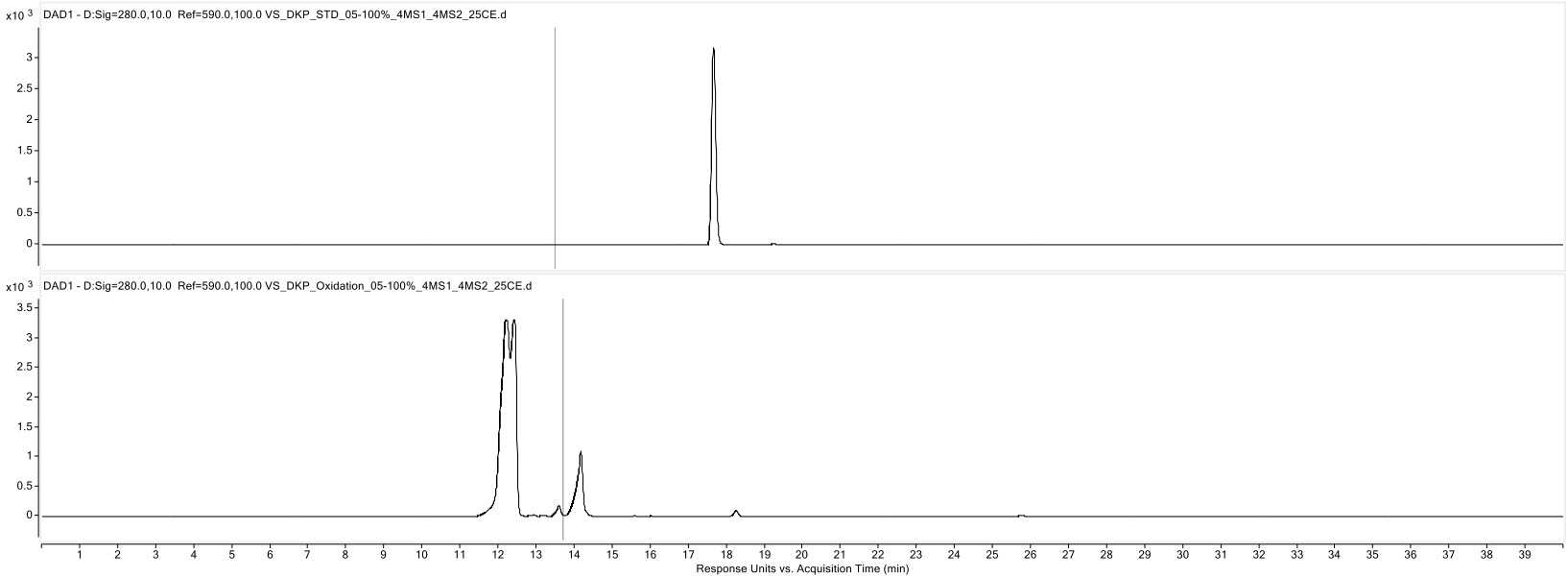

From top to bottom: standard for DKP **10**, crude reaction mixture showing benzothiophene sulfone at 14 min and **11**/**11'** at 12 min.

Supplementary Figure S12. Representative preparatory HPLC spectra (254 nm) for **11** and **11'**.

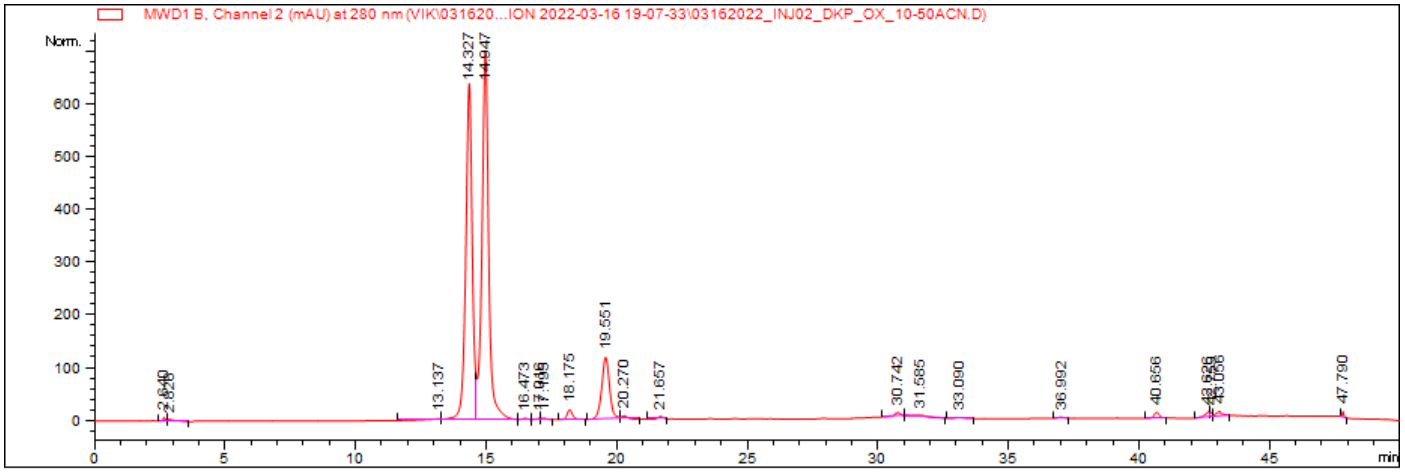

Major peaks at 14 minutes are **11**/**11'**, benzothiophene sulfone at 19.5 min and remaining starting material **10** at 31.5 minutes.

Supplementary Figure S13. Overlaid HPLC traces for purified **11'** (black) and **11** (red).

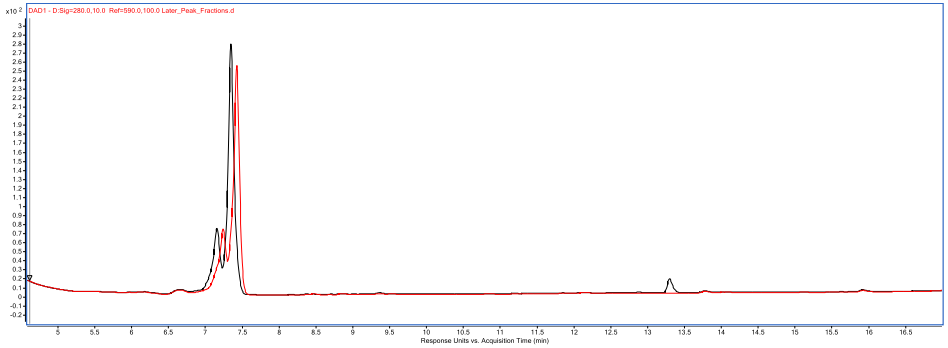

Supplementary Figure S14. Mass spectra for purified **11'**, **11**, and benzothiophene sulfone.

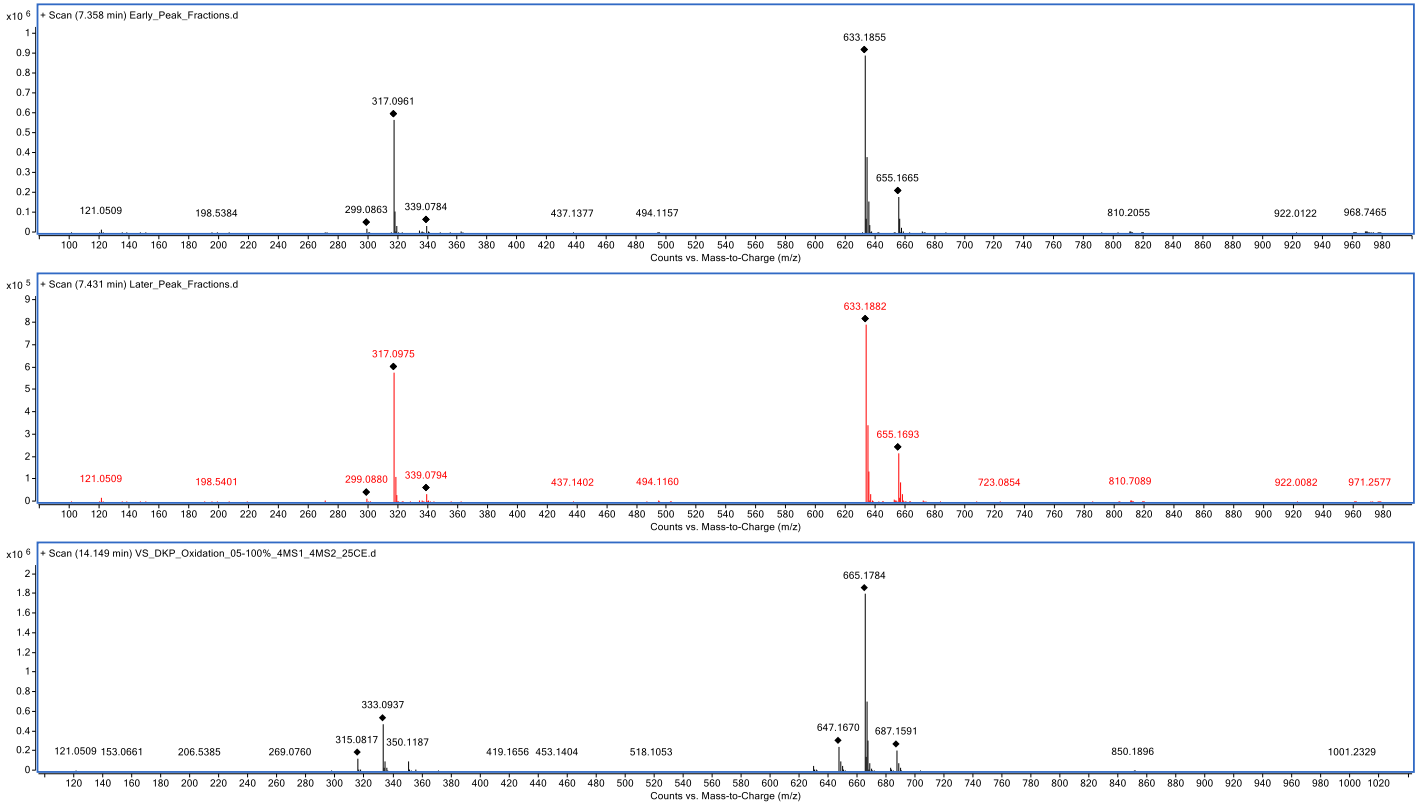

From top to bottom: Mass spectra for purified **11'**, **11**, and benzothiophene sulfone.

Supplementary Figure S15. LC-MS spectra (254 nm) for reactions of **10** with P450s.

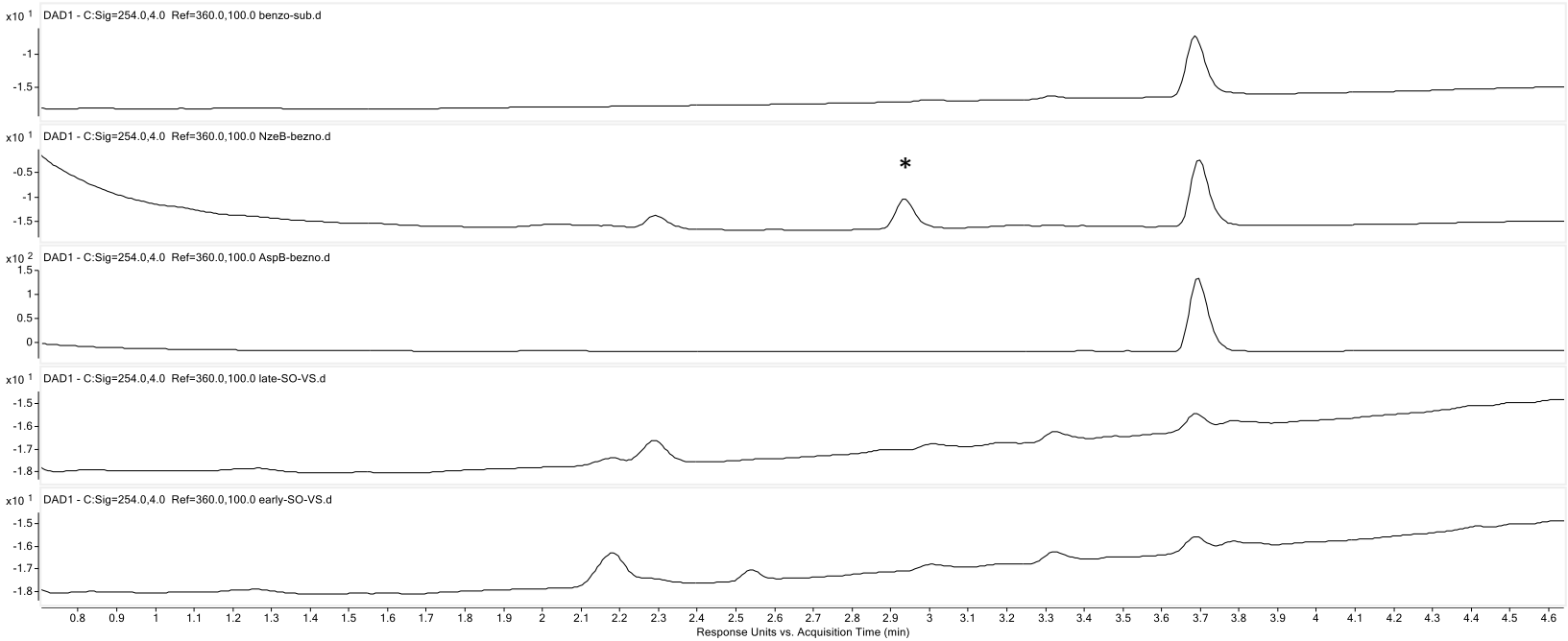

From top to bottom: **10** standard, reaction of **10** with NzeB, reaction of **10** with AspB, purified standard of diastereomer **11** that co-elutes with products formed by C–C bond forming P450s, purified standard of diastereomer **11'** that does not co-elute with products formed by C–C bond forming P450s.*Asterisk corresponds to M+32 mass of sulfone.

Supplementary Figure S16. LC-MS spectra (TIC) for reactions with **10** and P450s.

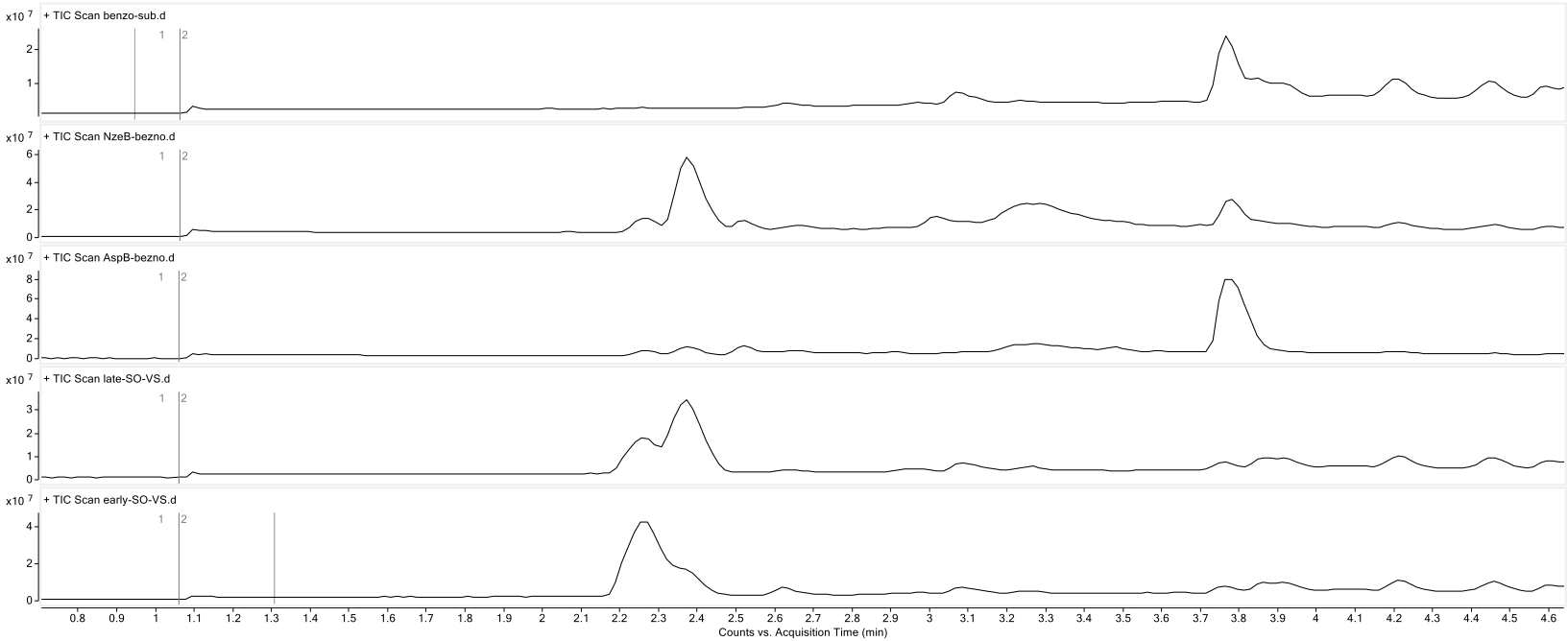

From top to bottom: **10** standard, reaction of **10** with NzeB, reaction of **10** with AspB, purified standard of diastereomer **11** that co-elutes with products formed by C–C bond forming P450s, purified standard of diastereomer **11'** that does not co-elute with products formed by C–C bond forming P450s.

Supplementary Figure S17. Selected MS spectra from reactions of **10** with P450s.

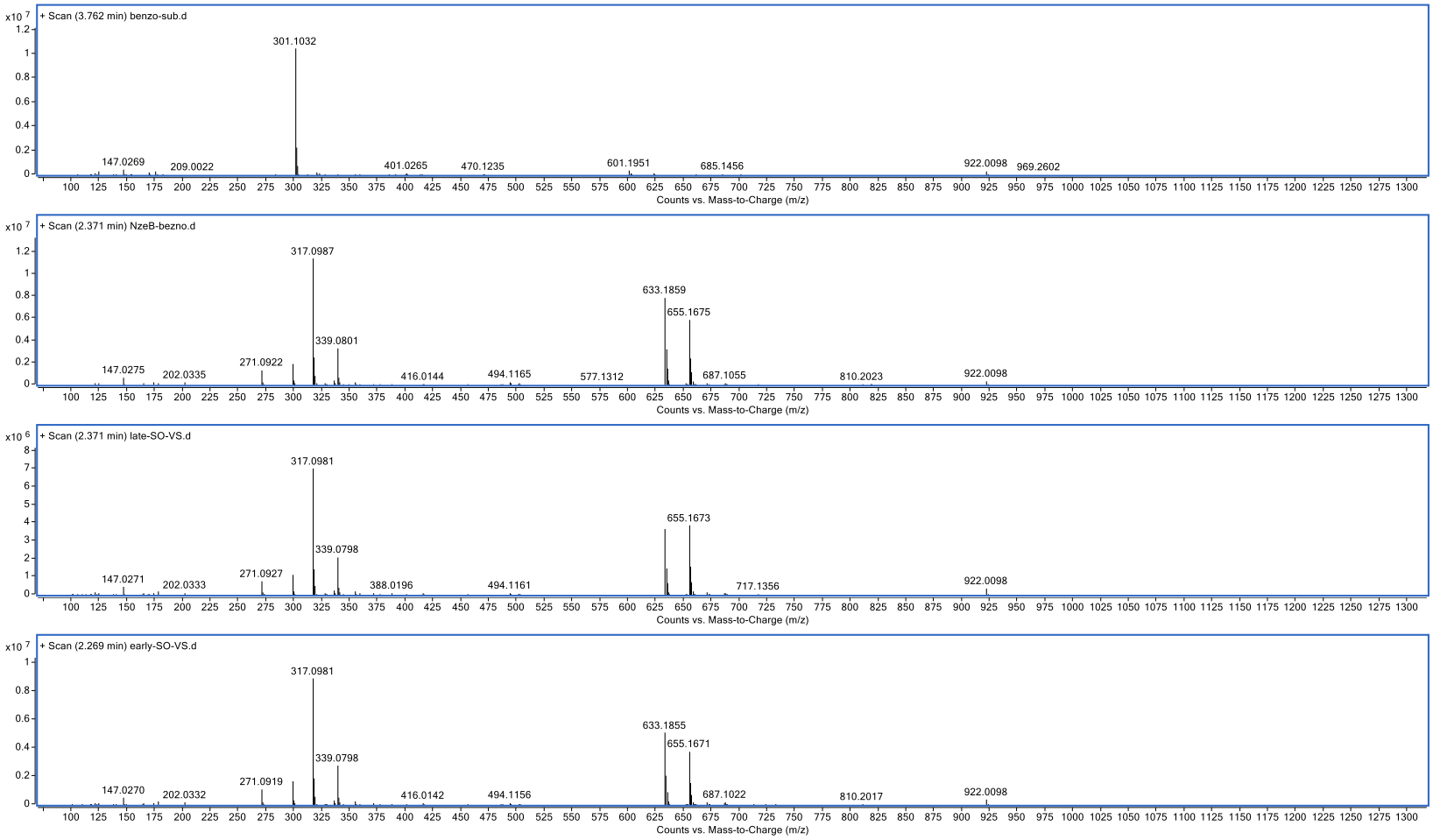

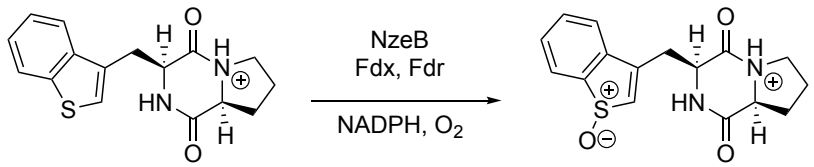

10
Exact Mass: 301.1005

11
Exact Mass: 317.0954

From top to bottom: **10** standard, reaction of **10** with NzeB, purified standard of diastereomer **11** that co-elutes with products formed by C–C bond forming P450s, purified standard of diastereomer **11'** that does not co-elute with products formed by C–C bond forming P450s.

Supplementary Figure S18. LC-MS spectra (254 nm) for reactions of **S1** with P450s.

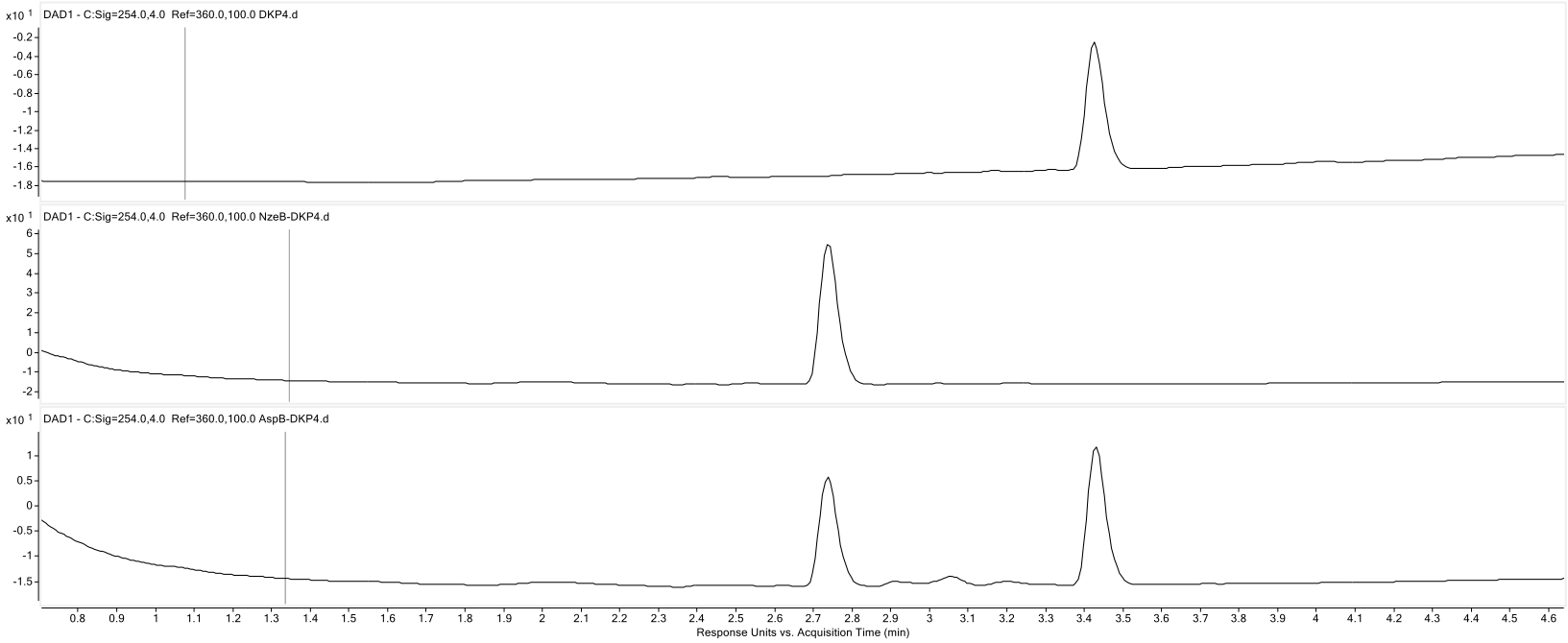

From top to bottom: **S1** standard, reaction of **S1** with NzeB, reaction of **S1** with AspB.

Supplementary Figure S19. LC-MS spectra (TIC) for reactions with **S1** and P450s.

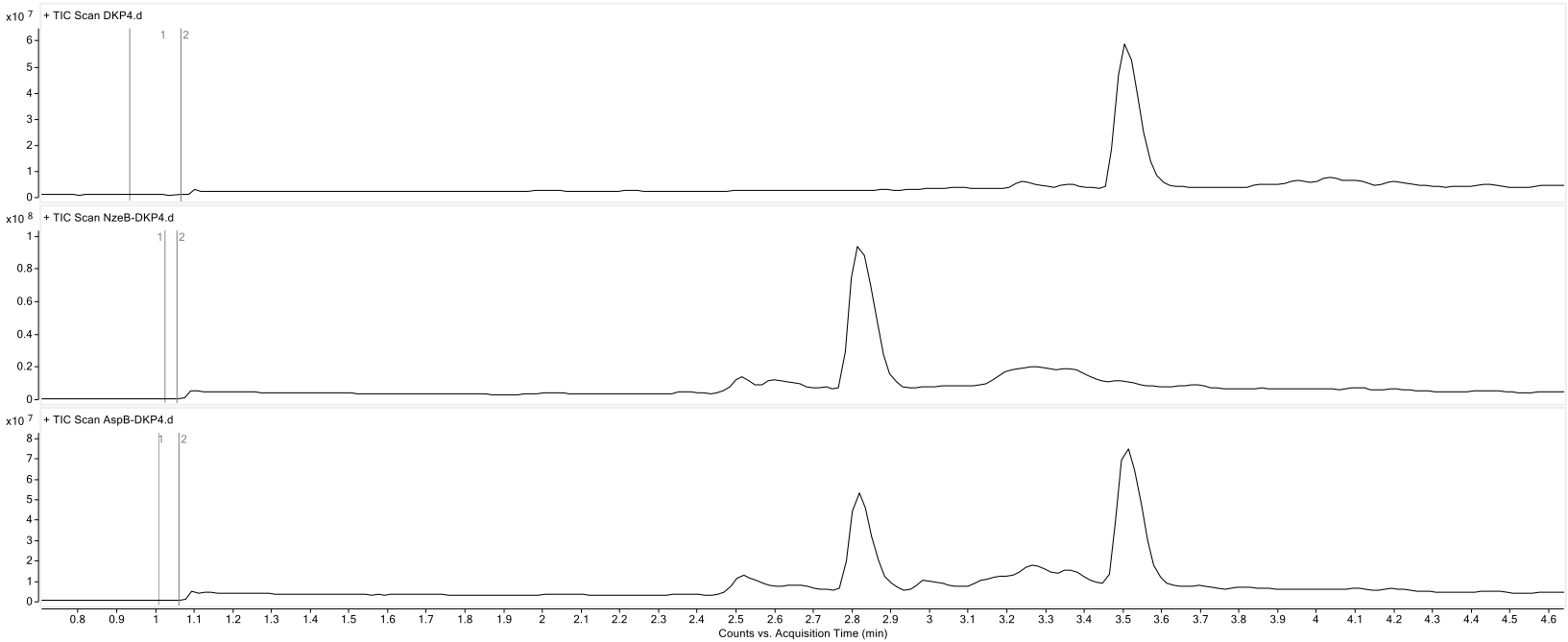

From top to bottom: **S1** standard, reaction of **S1** with NzeB, reaction of **S1** with AspB.

Supplementary Figure S20. Selected MS spectra from reactions of **S1** with P450s.

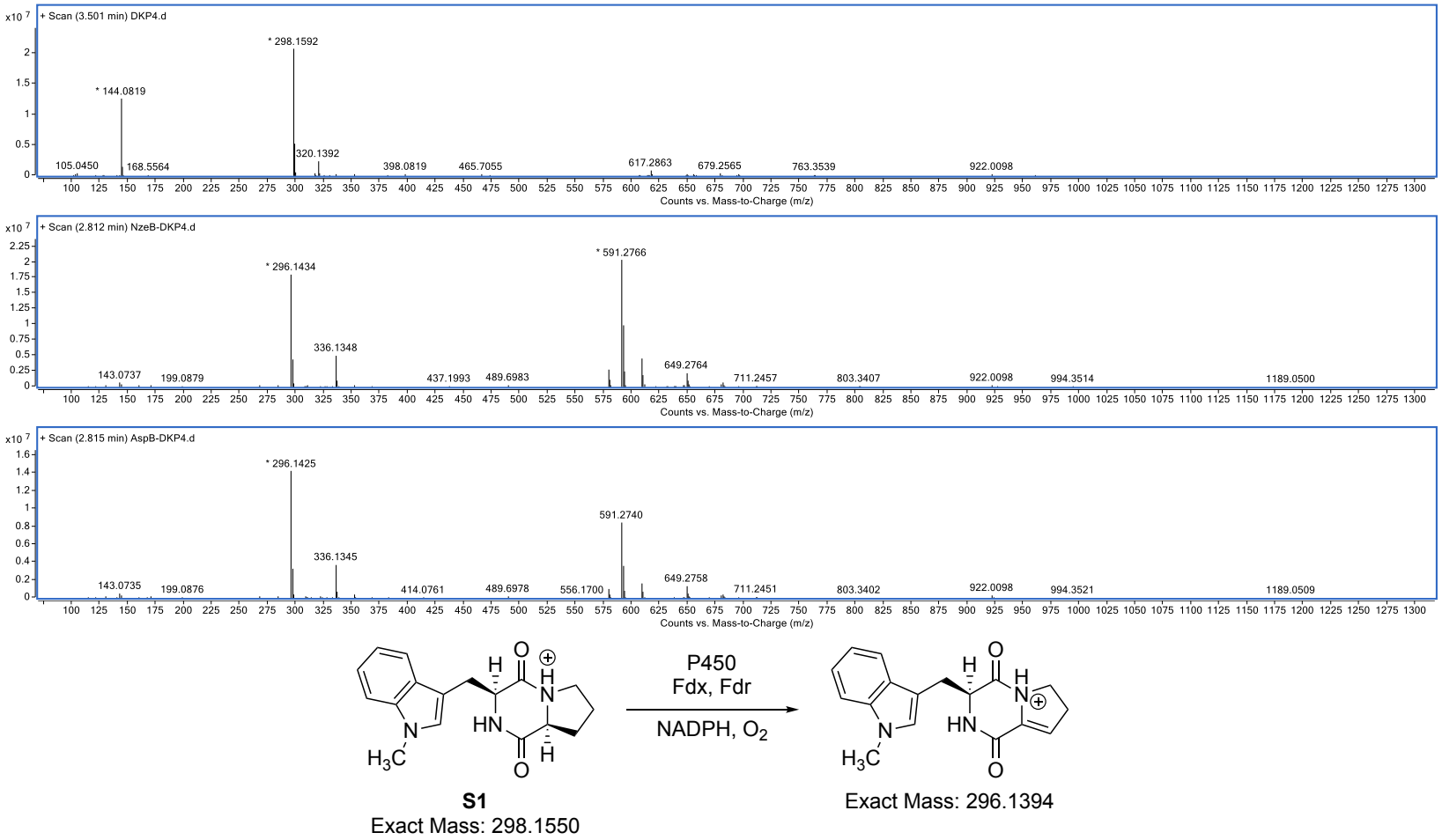

From top to bottom: **S1** standard, reaction of **S1** with NzeB, reaction of **S1** with AspB. Mass of **S1** and generic structure and mass of an observed dehydrogenated product.

Supplementary Figure S21. LC-MS spectra (254 nm) for reactions of **S2** with P450s.

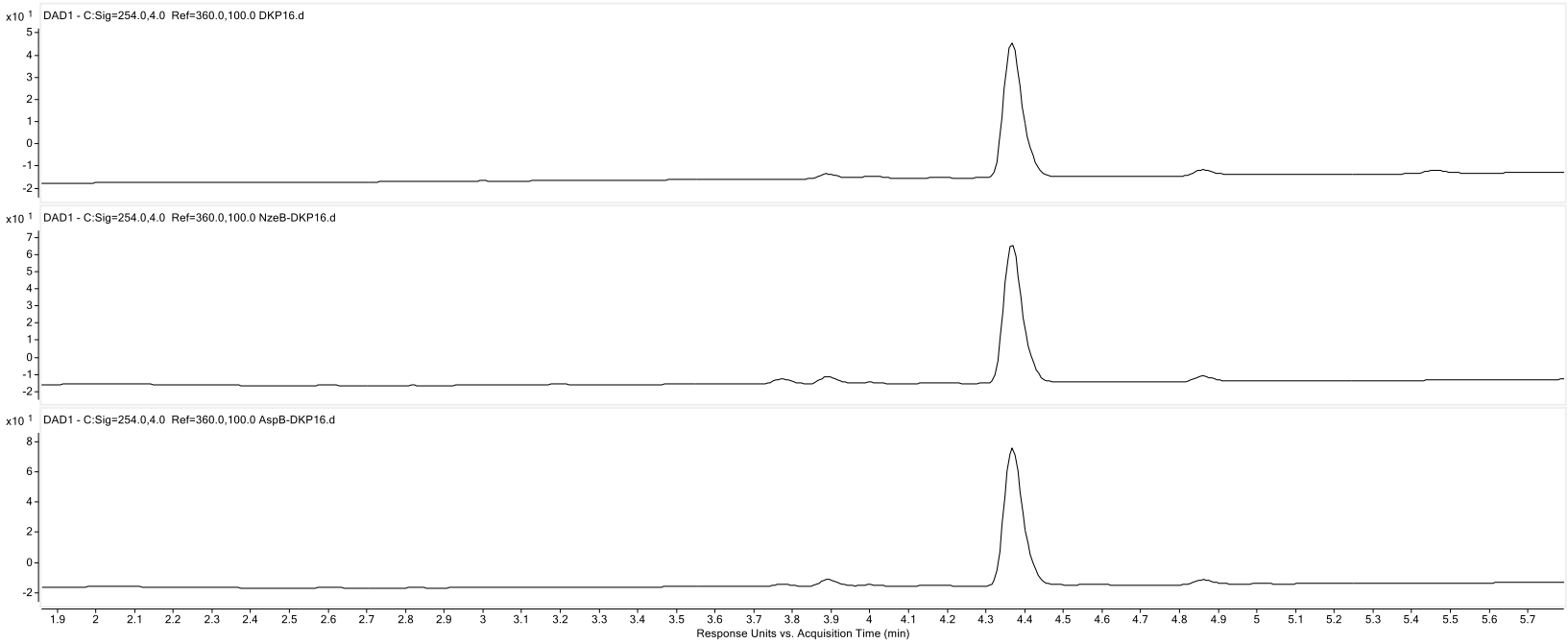

From top to bottom: **S2** standard, reaction of **S2** with NzeB, reaction of **S2** with AspB.

Supplementary Figure S22. LC-MS spectra (TIC) for reactions with **S2** and P450s.

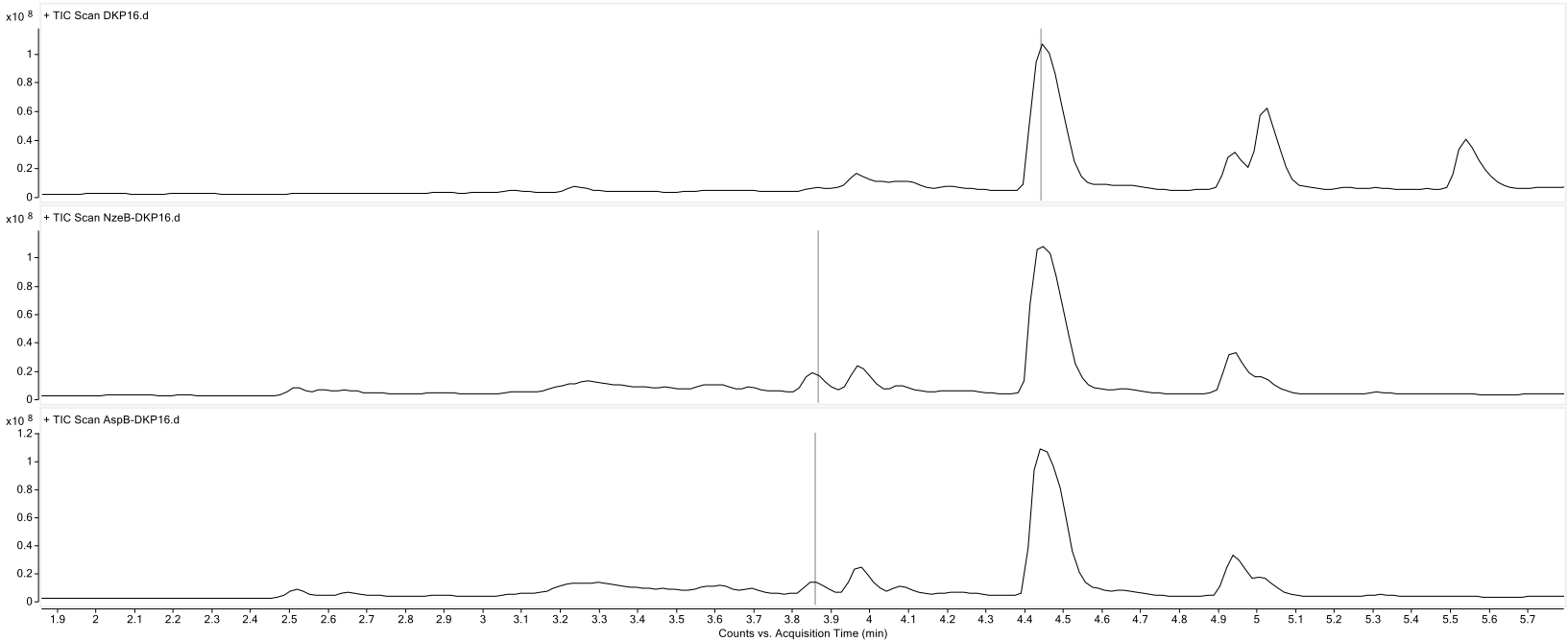

From top to bottom: **S1** standard, reaction of **S1** with NzeB, reaction of **S2** with AspB.

Supplementary Figure S23. Selected MS spectra from reactions of **S2** with P450s.

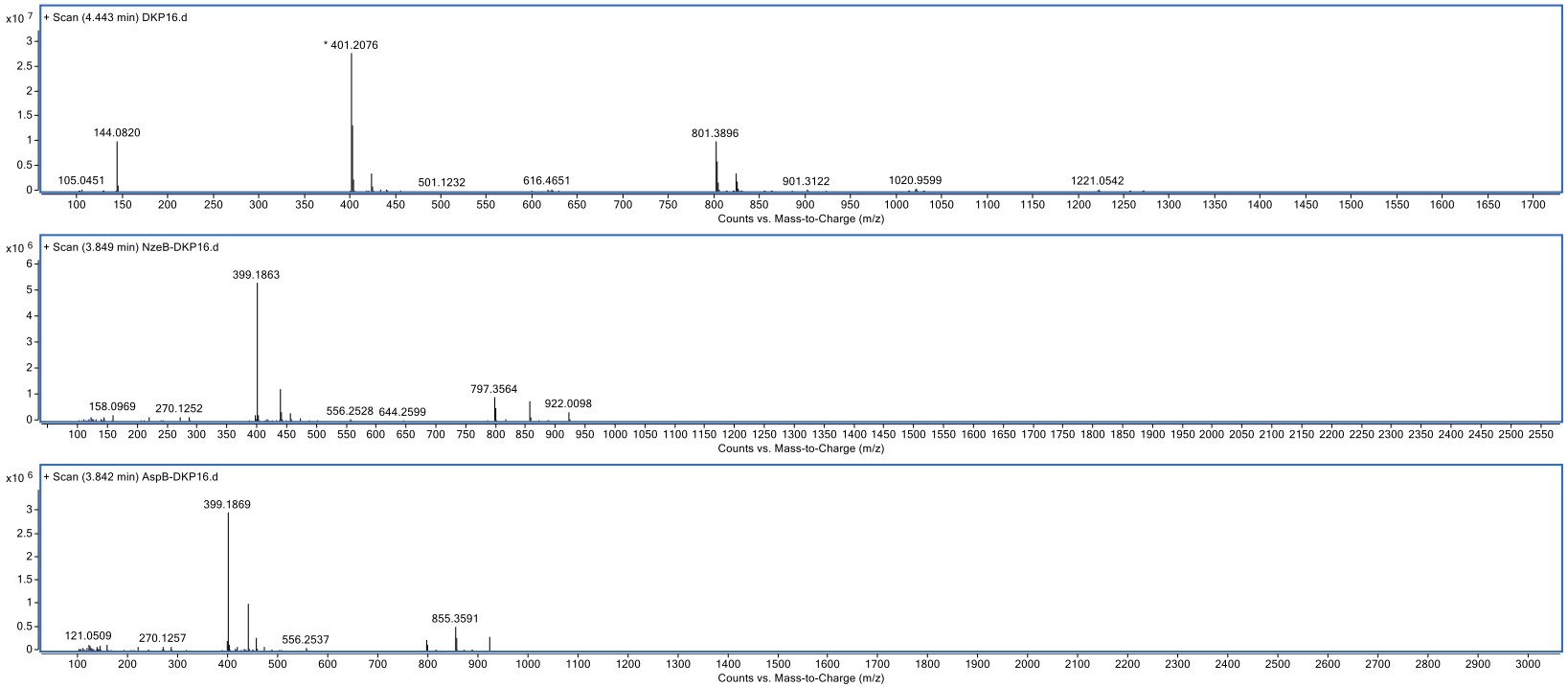

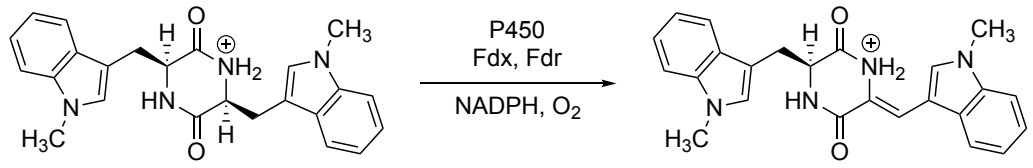

S2
Exact Mass: 401.1972

Exact Mass: 399.1816

From top to bottom: **S2** standard, reaction of **S2** with NzeB, reaction of **S1** with AspB. Mass of **S2** and generic structure and mass of an observed dehydrogenated product.

Supplementary Figure S24. ^{1}H NMR spectra of **S1** in DMSO-d_6.

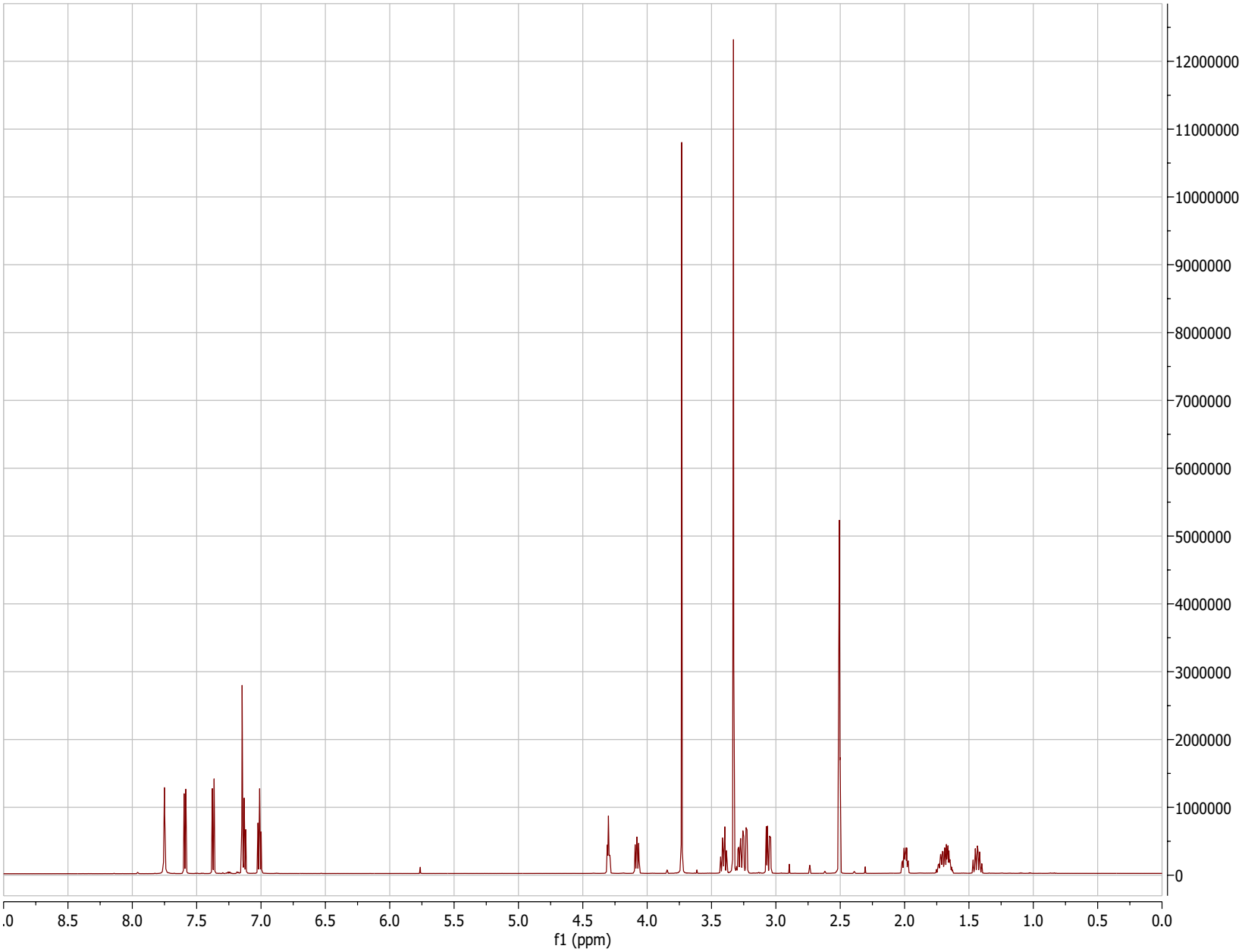

Supplementary Figure S25. ^{13}C NMR spectra of **S1** in DMSO-d_6.

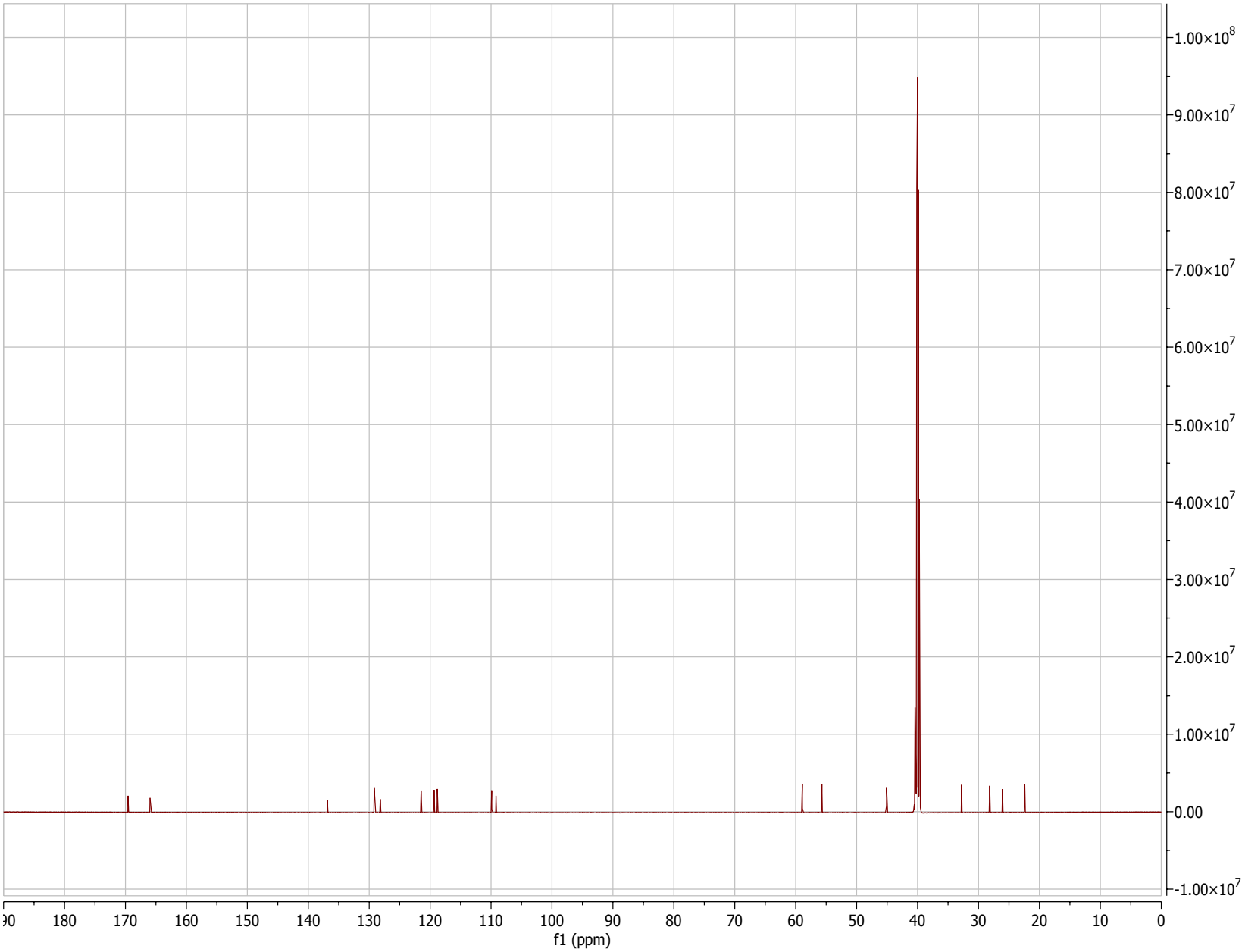

Supplementary Figure S26. ^{1}H NMR spectra of **S2** in DMSO-d_6.

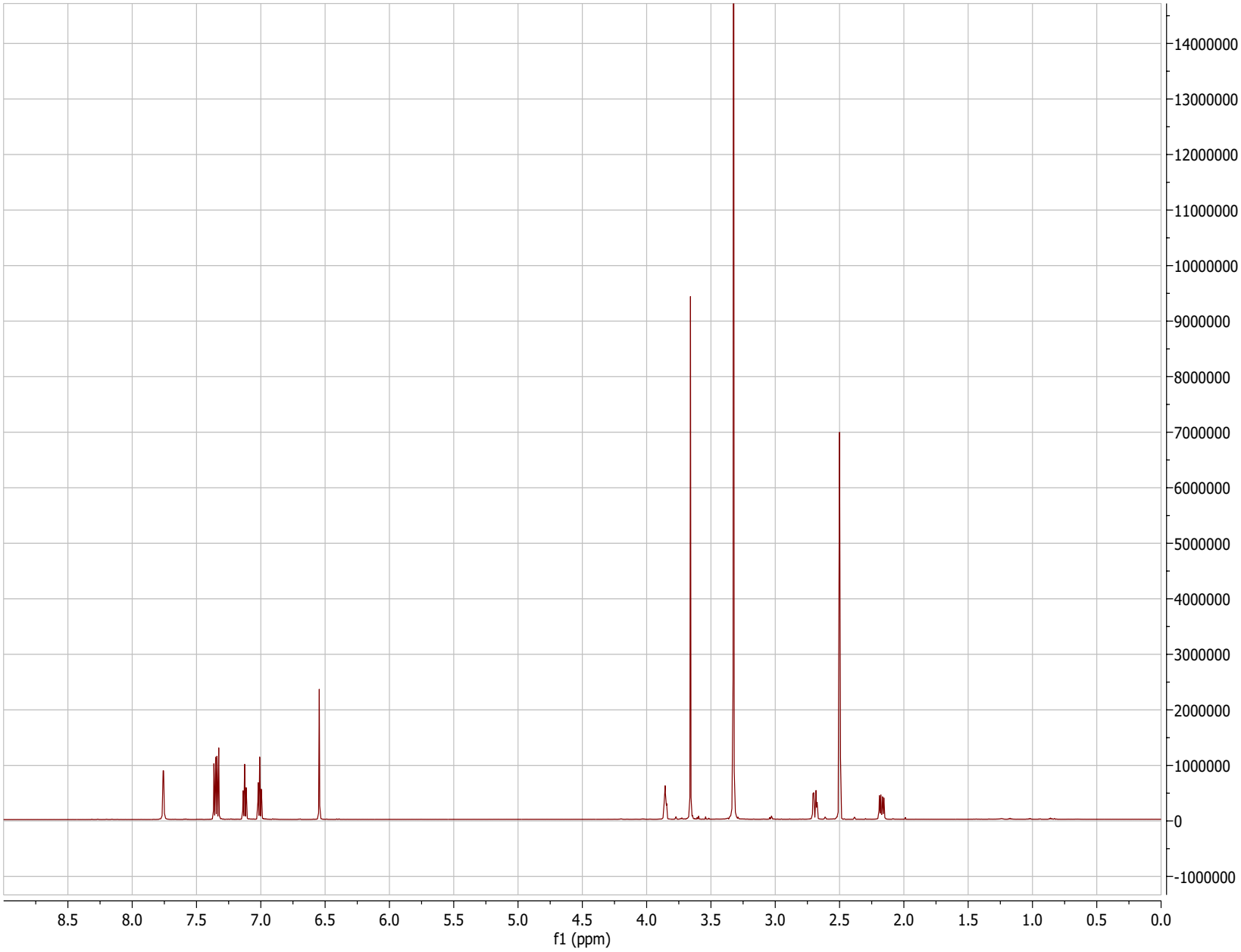

Supplementary Figure S27. ^{13}C NMR spectra of **S2** in DMSO-d_6.

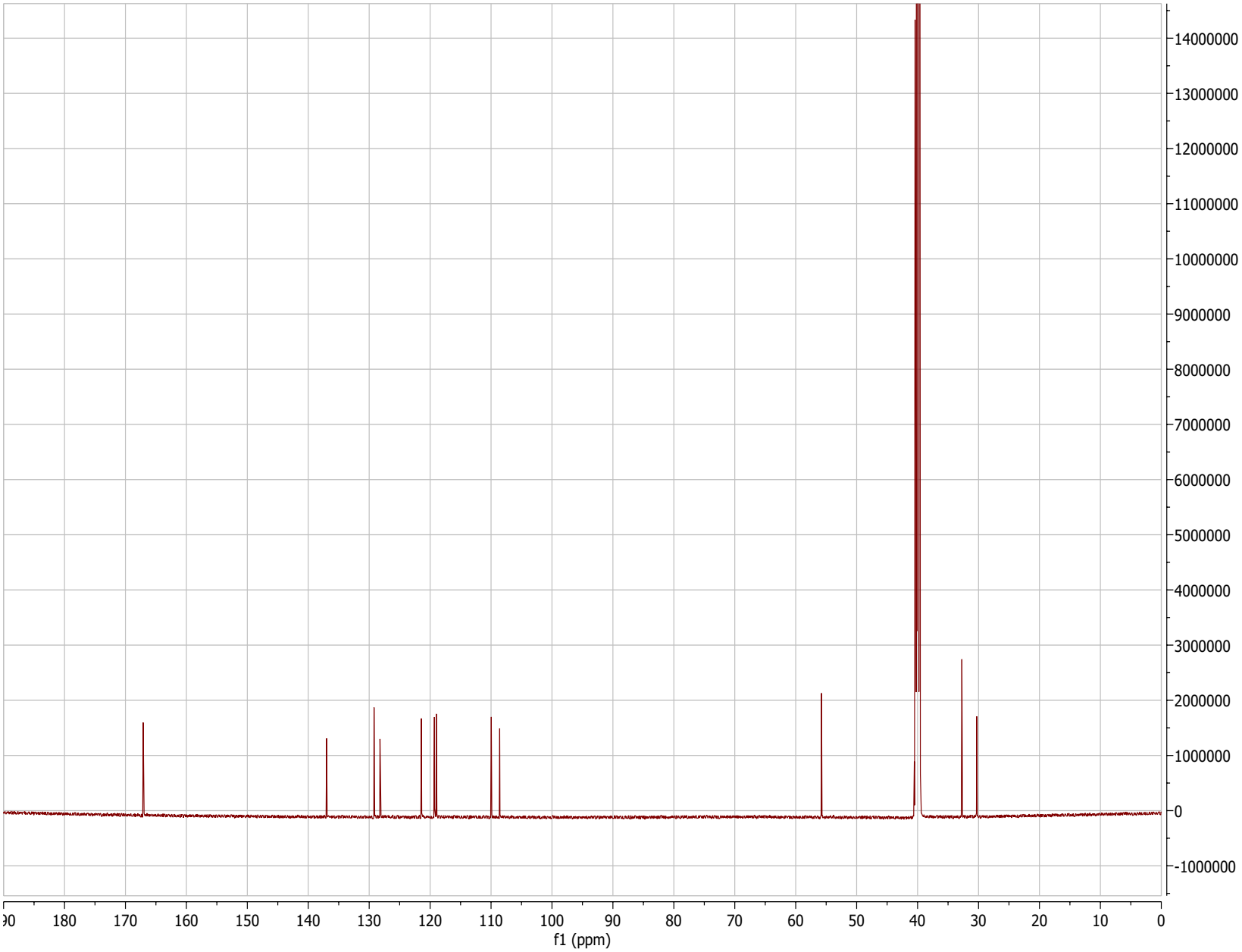

Supplementary Figure S28. ^{1}H NMR spectra of **10** in $CDCl_3$.

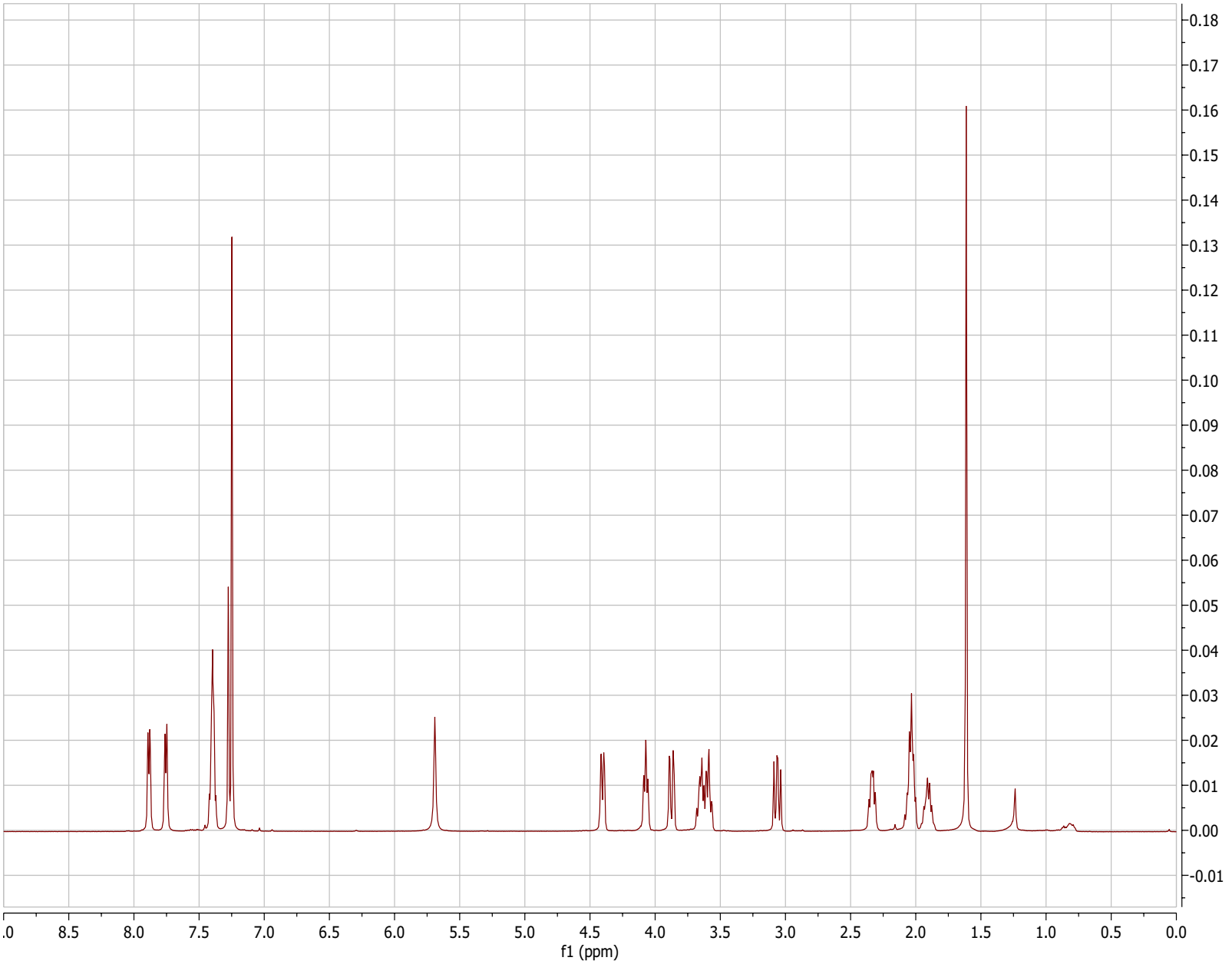

Supplementary Figure S29. ^{13}C NMR spectra of **10** in $CDCl_3$.

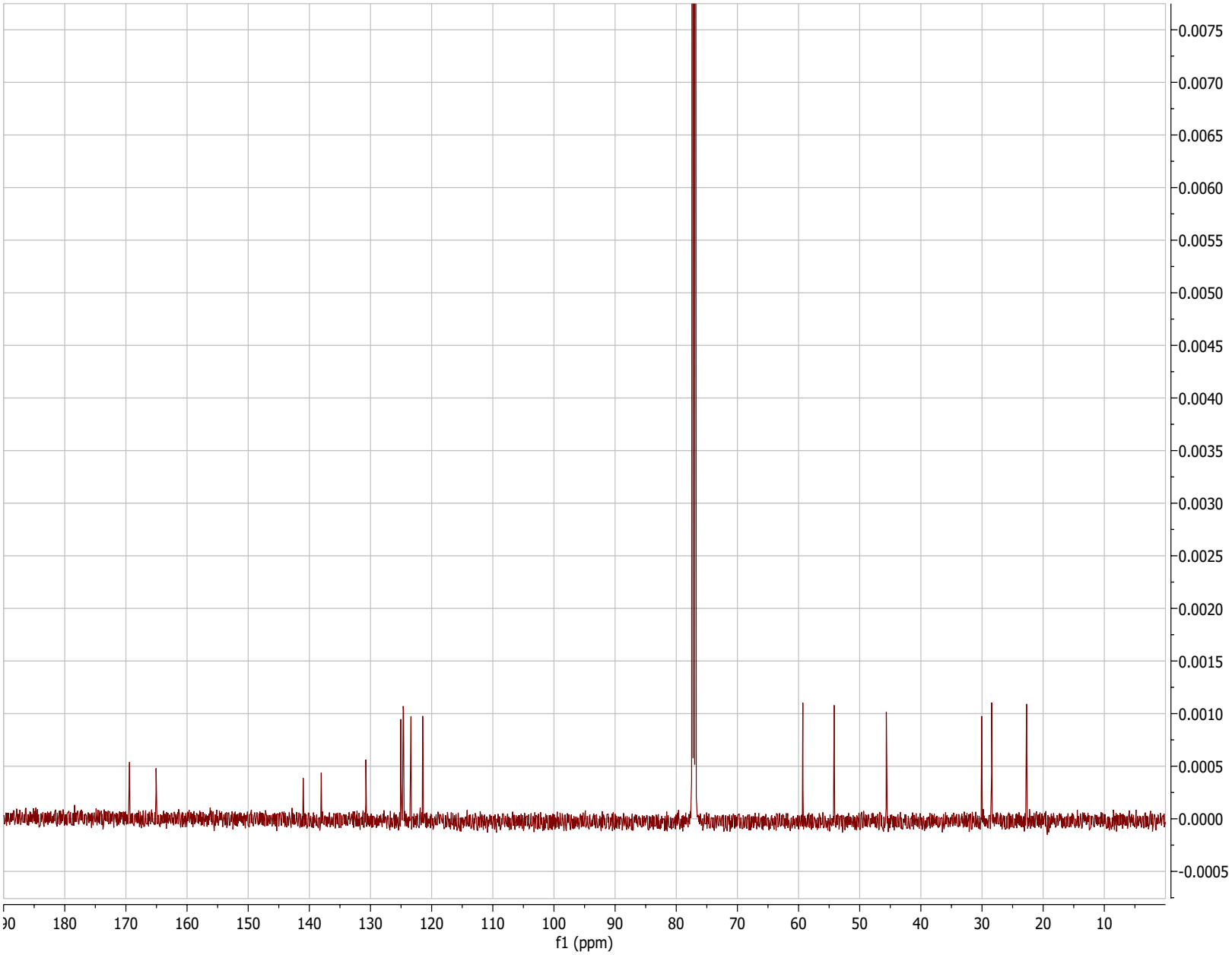

Supplementary Figure S30. ^{1}H NMR spectra of **11'** in $CDCl_3$.

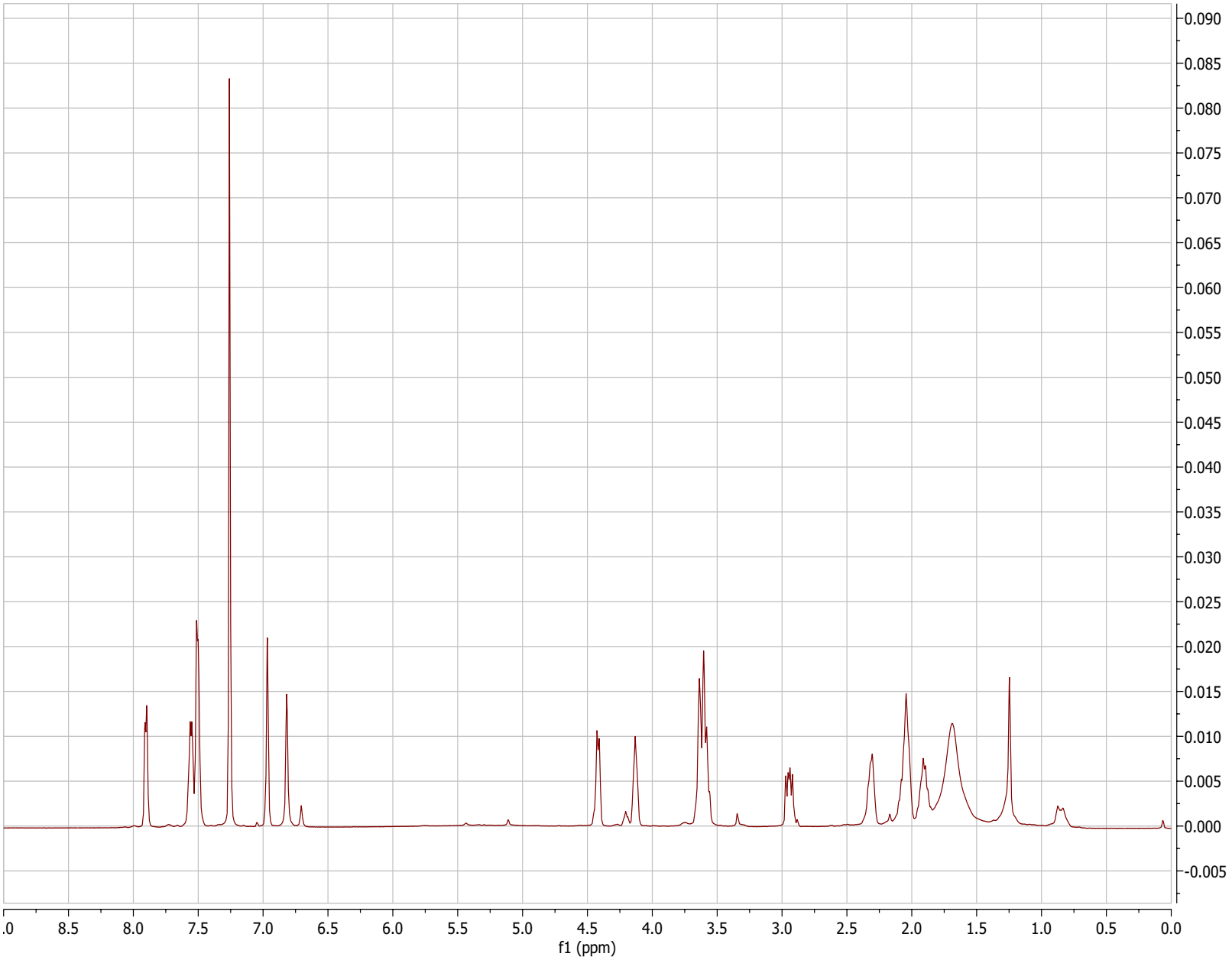

Supplementary Figure S31. ^{13}C NMR spectra of **11'** in $CDCl_3$.

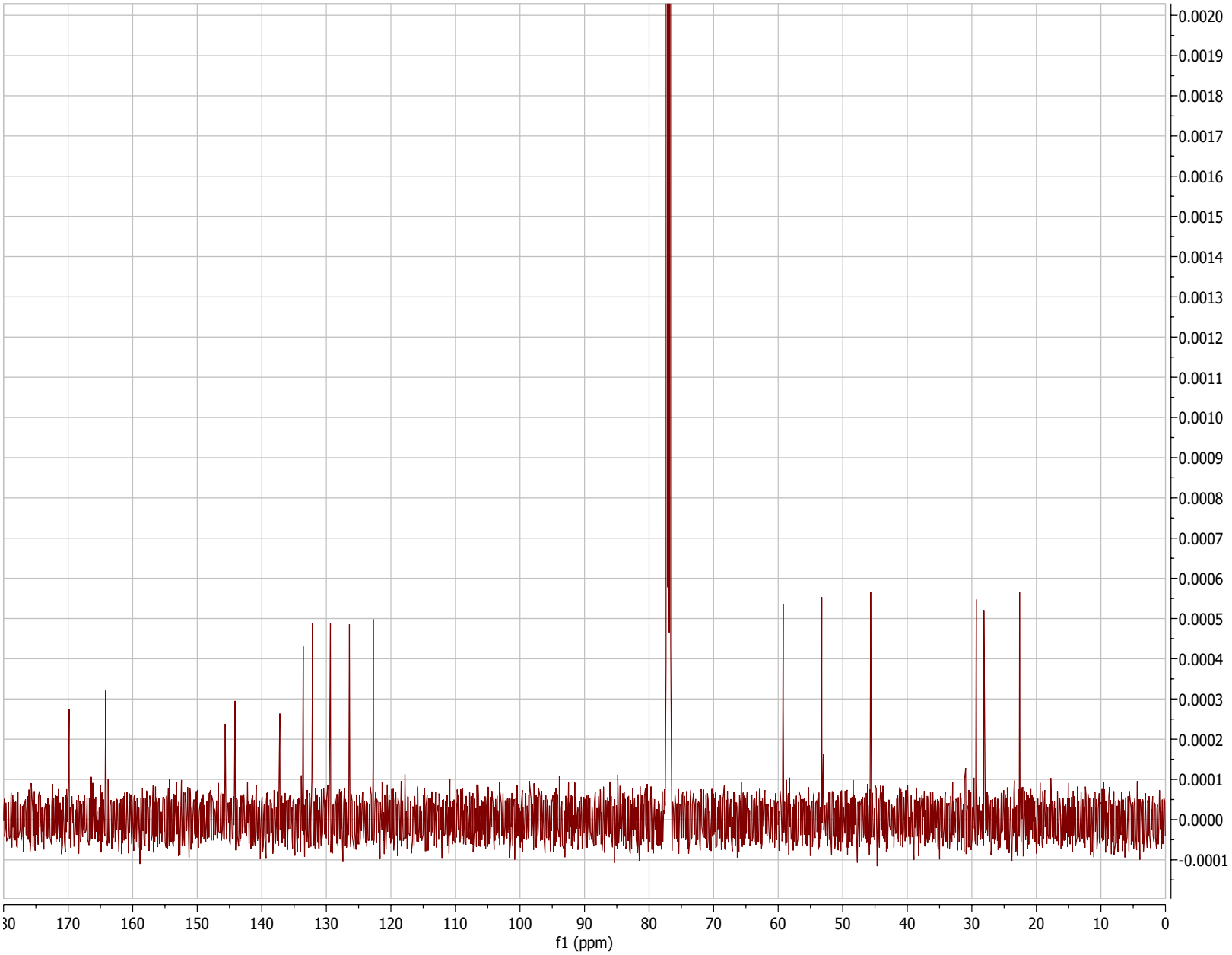

Supplementary Figure S32. ^{1}H NMR spectra of **11** in $CDCl_3$.

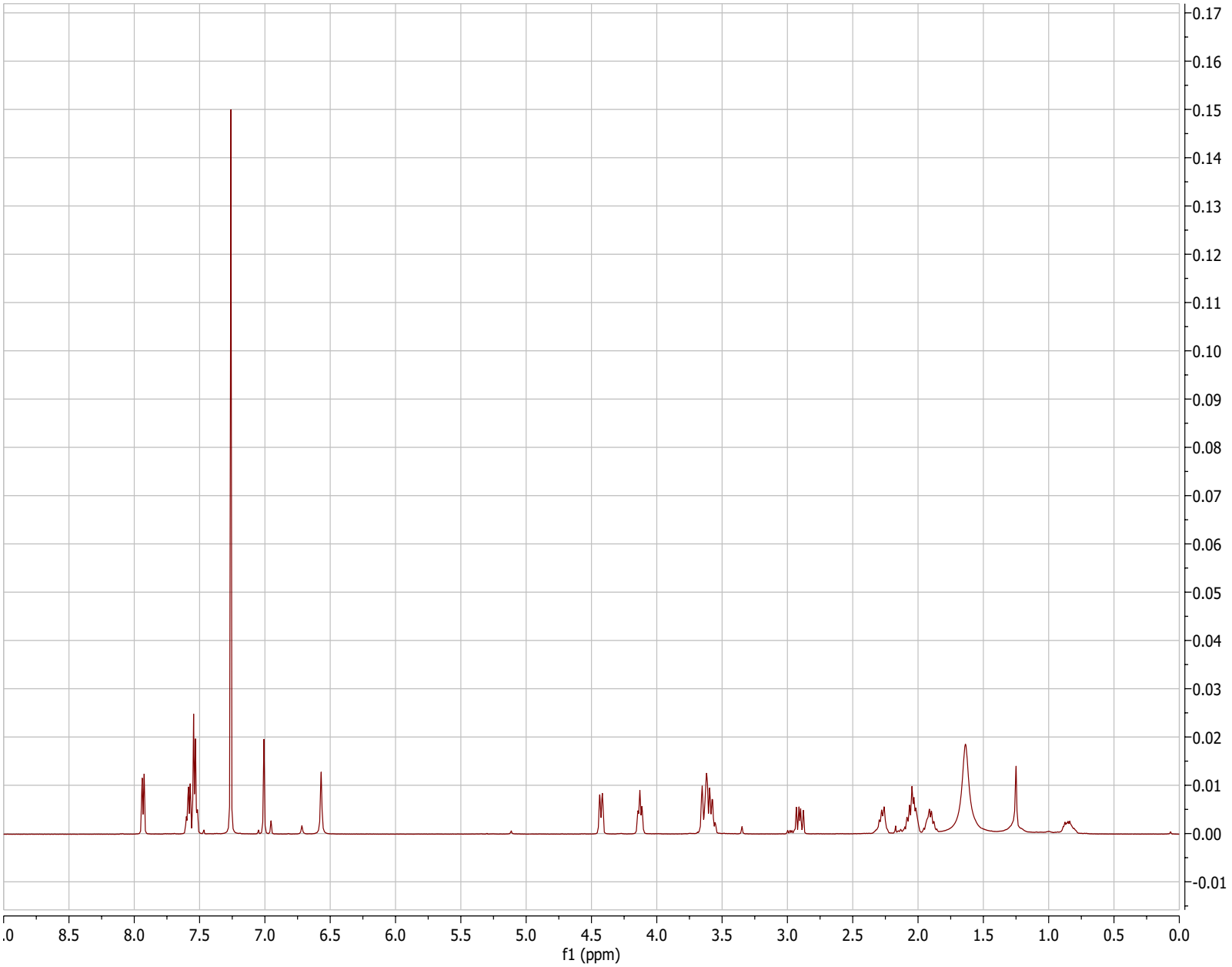

Supplementary Figure S33. ^{13}C NMR spectra of **11** in $CDCl_3$.

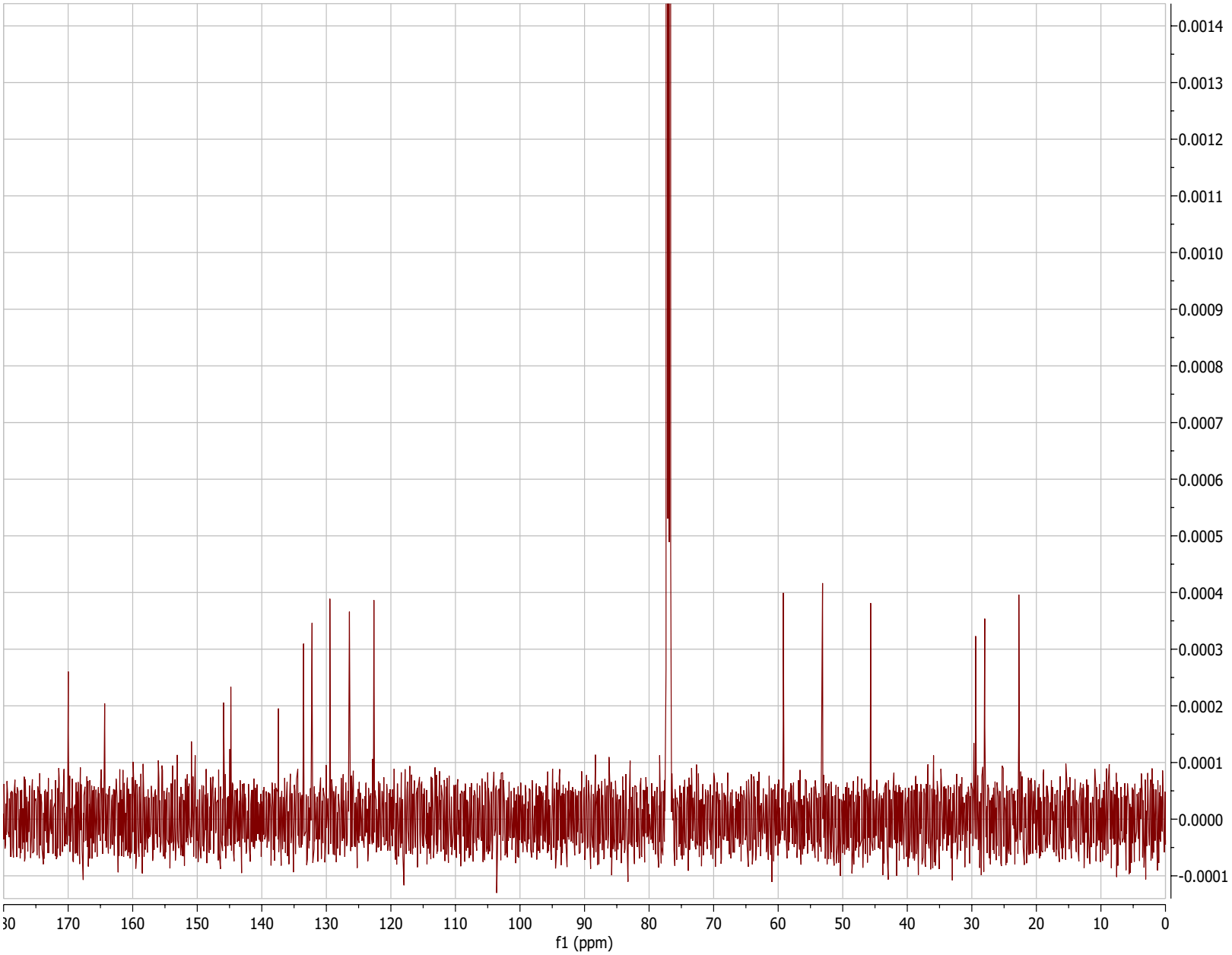

Supplementary Figure S34. Stacked ^{1}H NMR spectra of **11/11'** in $CDCl_3$.

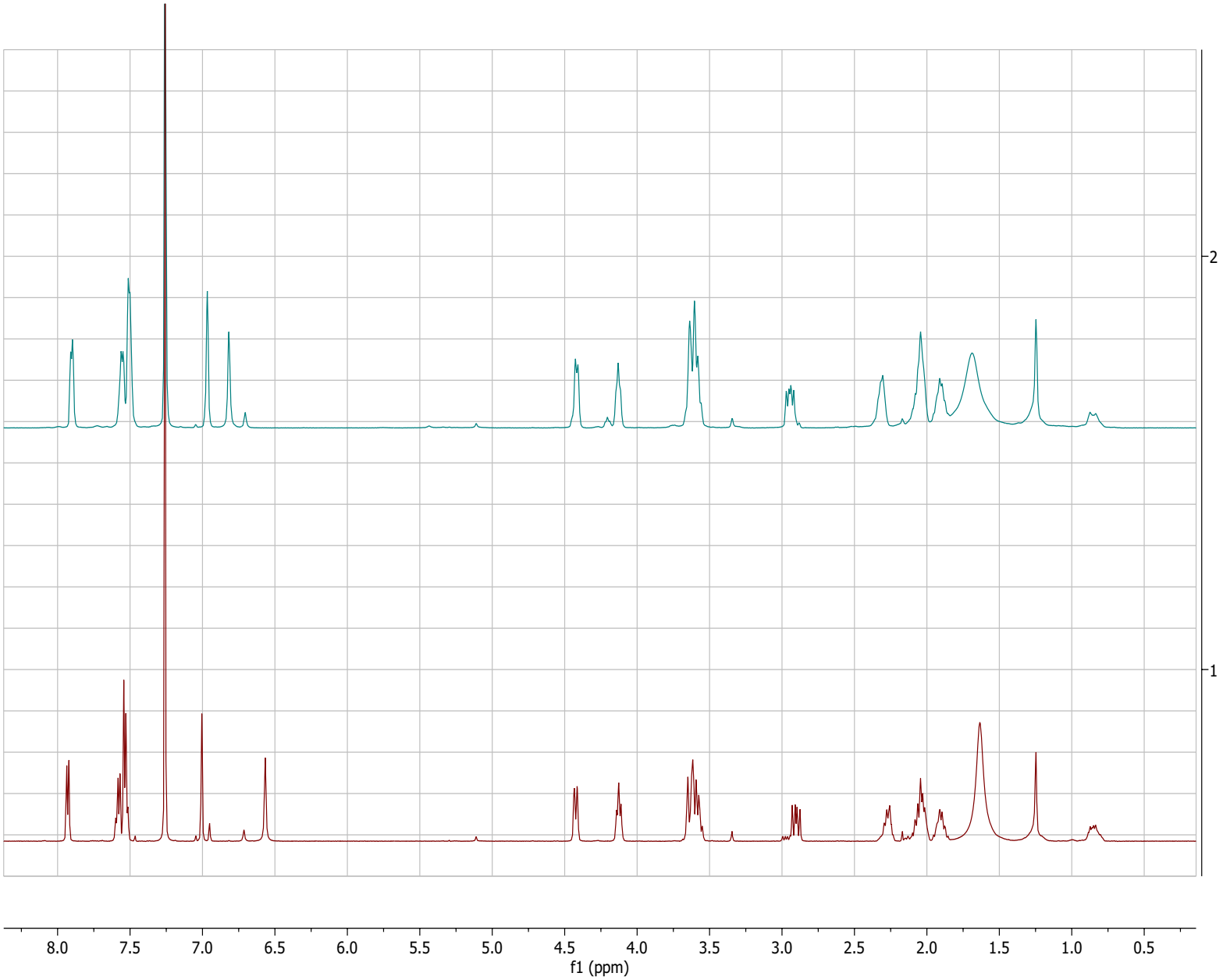

Upper spectra (aqua) = **11'**, lower spectra (red) = **11**.

Supplementary Figure S35. Stacked ^{1}H NMR spectra of **11/11'** in $CDCl_3$ (6.2-8.2 ppm).

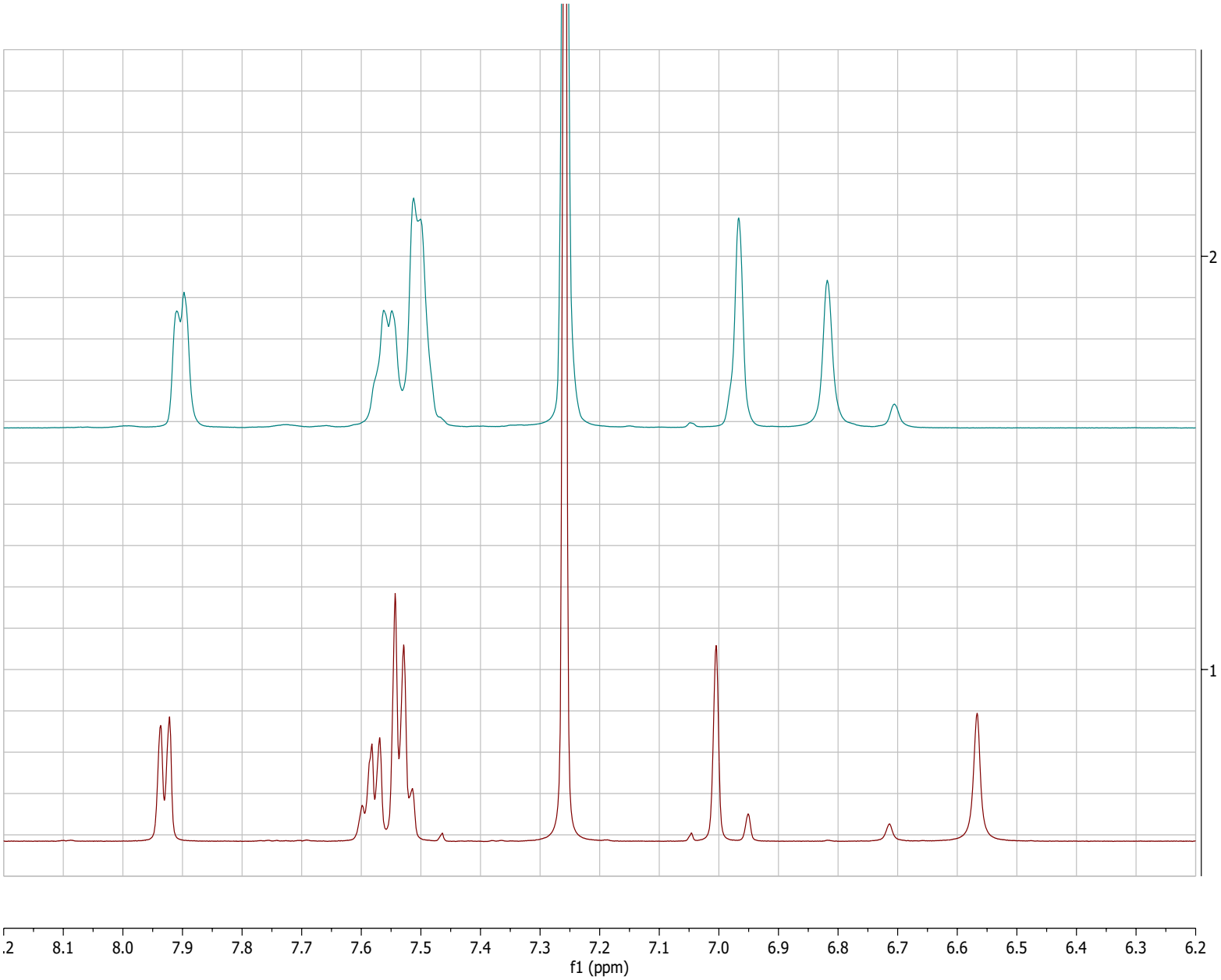

Upper spectra (aqua) = **11'**, lower spectra (red) = **11**.

Supplementary Figure S36. Stacked ^{13}C NMR spectra of **11/11'** in $CDCl_3$.

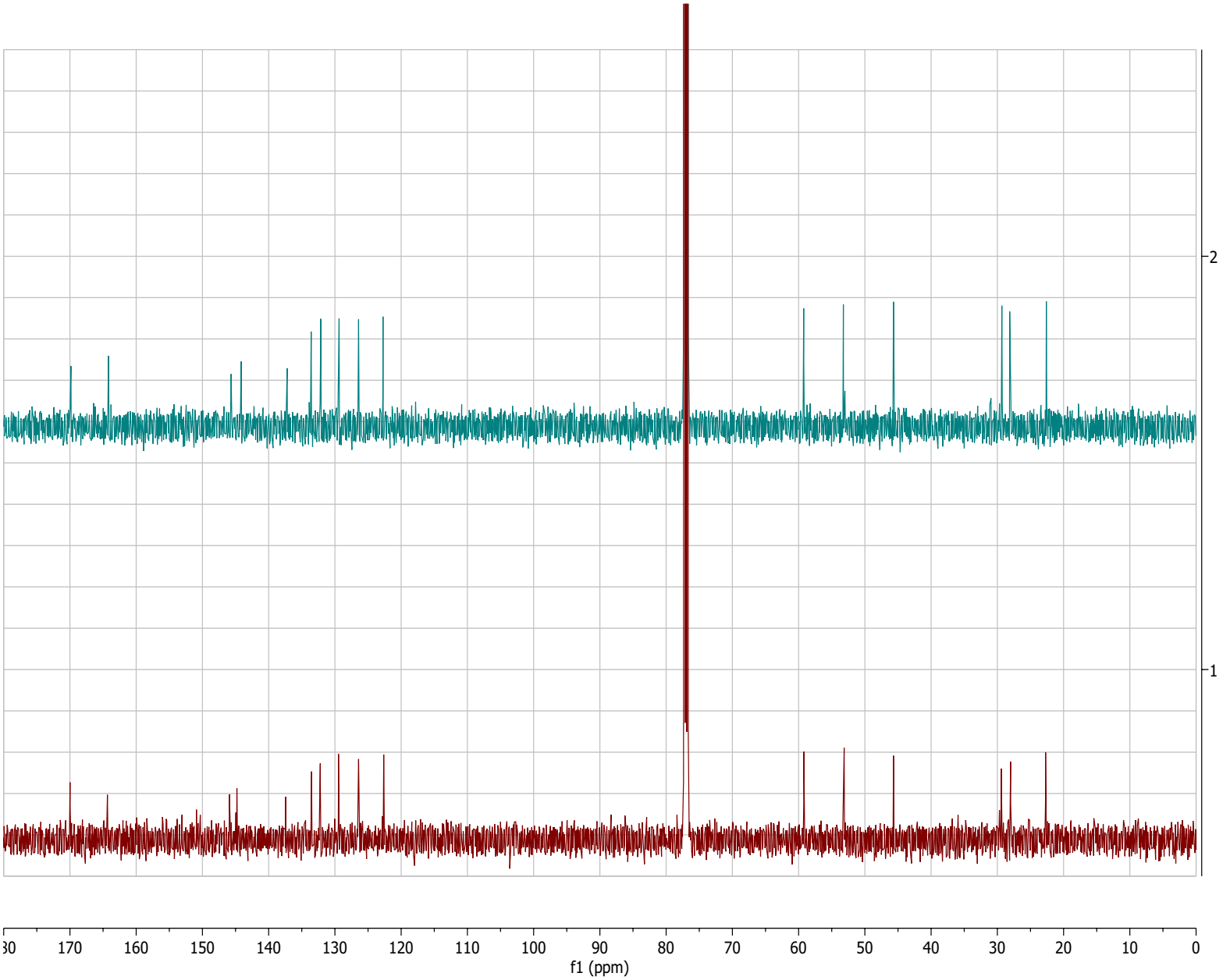

Upper spectra (aqua) = **11'**, lower spectra (red) = **11**.

Supplementary Figure S37. Stacked ^{13}C NMR spectra of **11/11'** in $CDCl_3$ (130-175 ppm).

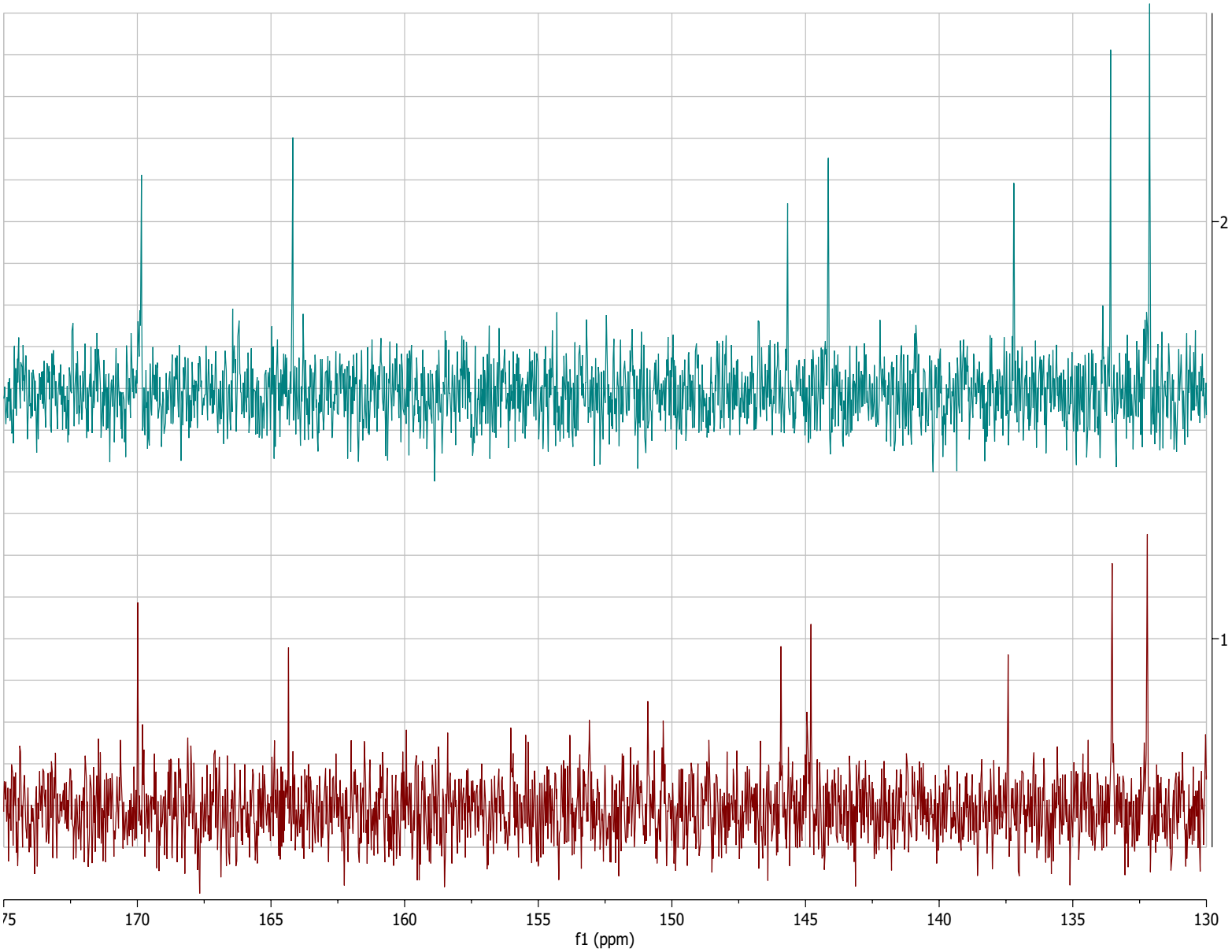

Upper spectra (aqua) = **11'**, lower spectra (red) = **11**.

Supplementary Figure S38. Stacked ^{13}C NMR spectra of **11/11'** in $CDCl_3$ (120-140 ppm).

Upper spectra (aqua) = **11'**, lower spectra (red) = **11**.

Supplementary Figure S39. Stacked ^{13}C NMR spectra of **11 and 10** in $CDCl_3$.

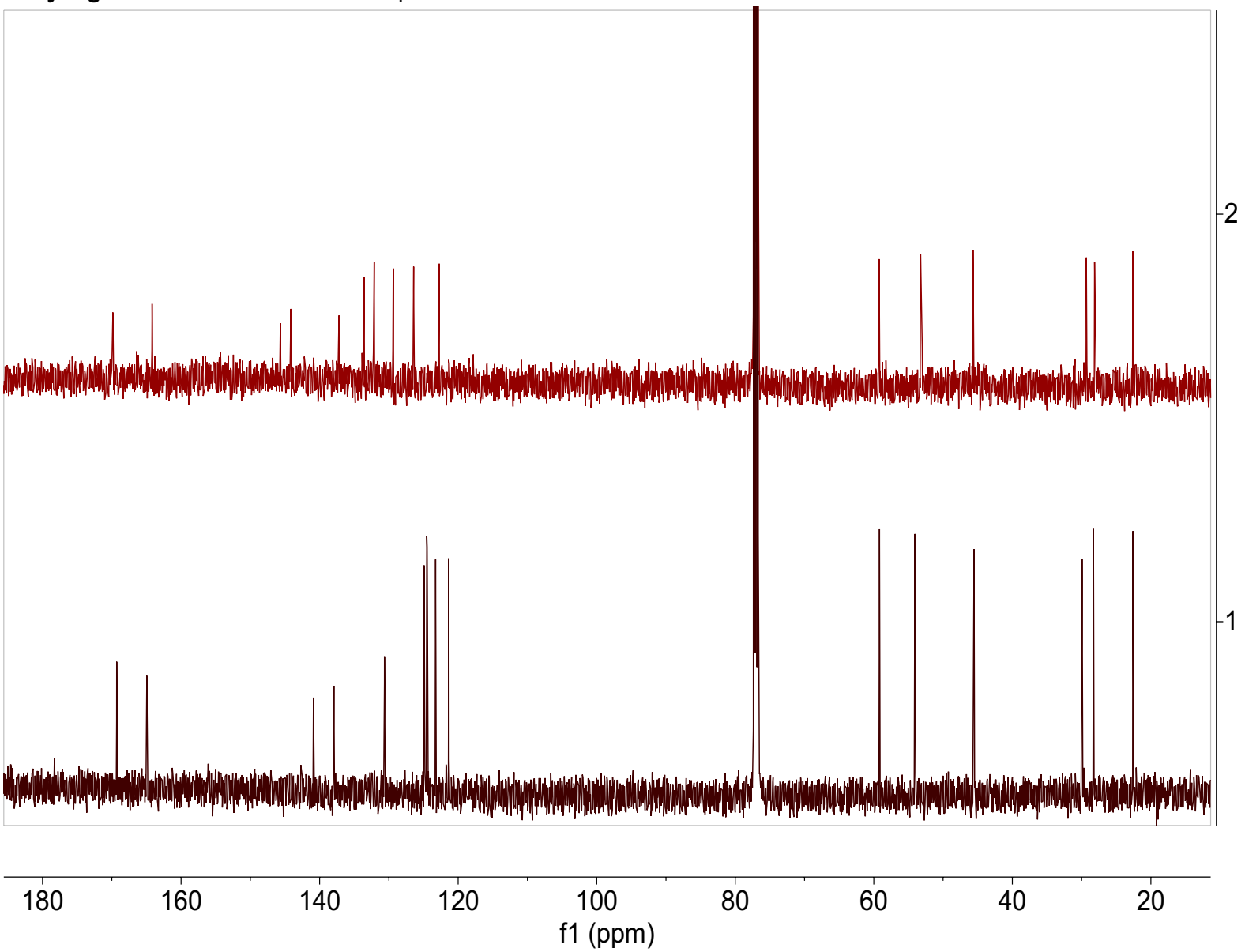

Upper spectra (red) = **11**, lower spectra (maroon) = **10**.

Note: the general shift of benzothiophene aromatic carbons downfield upon oxidation of benzothiophene to benzothiophene sulfoxide is in agreement with work from Saunders and coworkers.[25]

PerkinElmer Spectrum IR 10.6.2

5/20/2022 10:04:37 AM

Sample Details

Filename	Benzosubstrate
Creation Date	5/20/2022 9:51:07 AM
Analyst	Lab
X-Axis Units	cm-1
X-Axis start value	4000
X-Axis end value	650
Data interval	-1
Number of points	3351
Y-Axis Units	%T
Description	Sample 321 By Lab Date Friday, May 20 2022

Spectrum

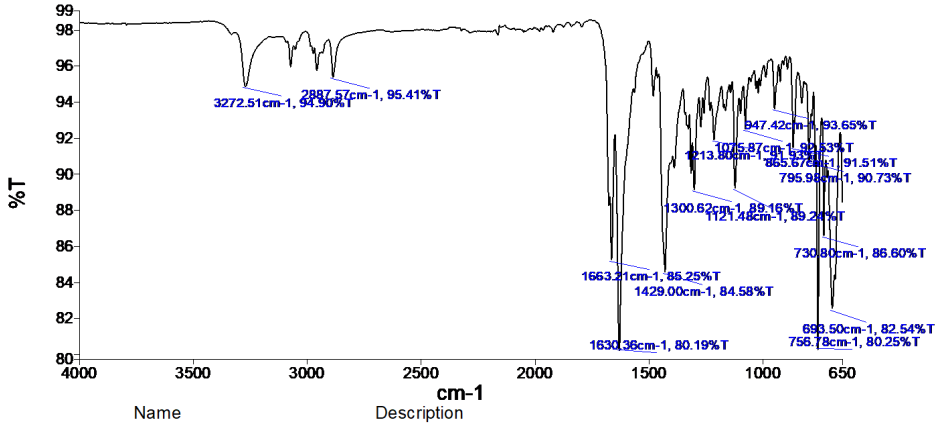

Peak Table Results

Result Spectrum

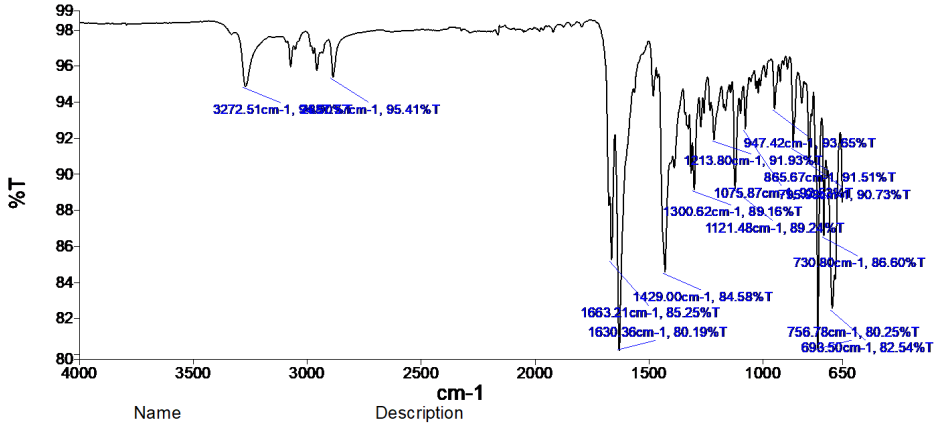

PerkinElmer Spectrum IR 10.6.2

5/20/2022 10:08:29 AM

Sample Details

Filename	Lateproduct
Creation Date	5/20/2022 9:56:05 AM
Analyst	Lab
X-Axis Units	cm-1
X-Axis start value	4000
X-Axis end value	650
Data interval	-1
Number of points	3351
Y-Axis Units	%T
Description	Sample 334 By Lab Date Friday, May 20 2022

Spectrum

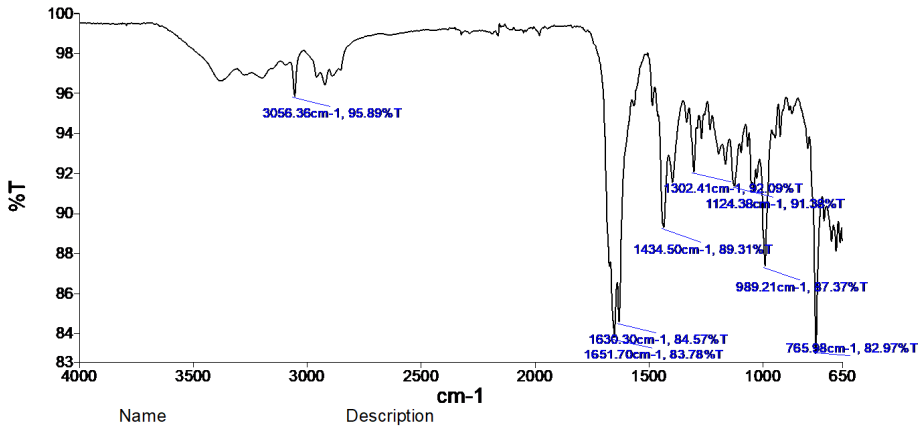

Peak Table Results

Result Spectrum

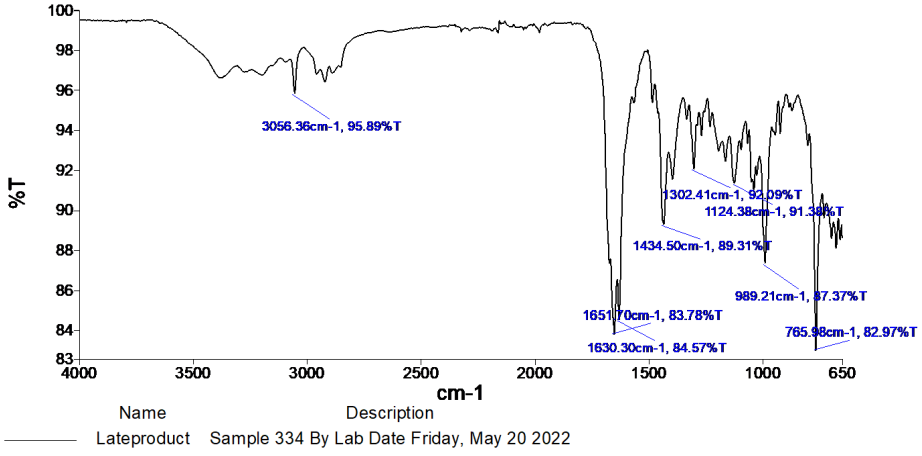

Supplementary Figure S42. Comparison of AlphaFold models to AspB and NzeB structures.

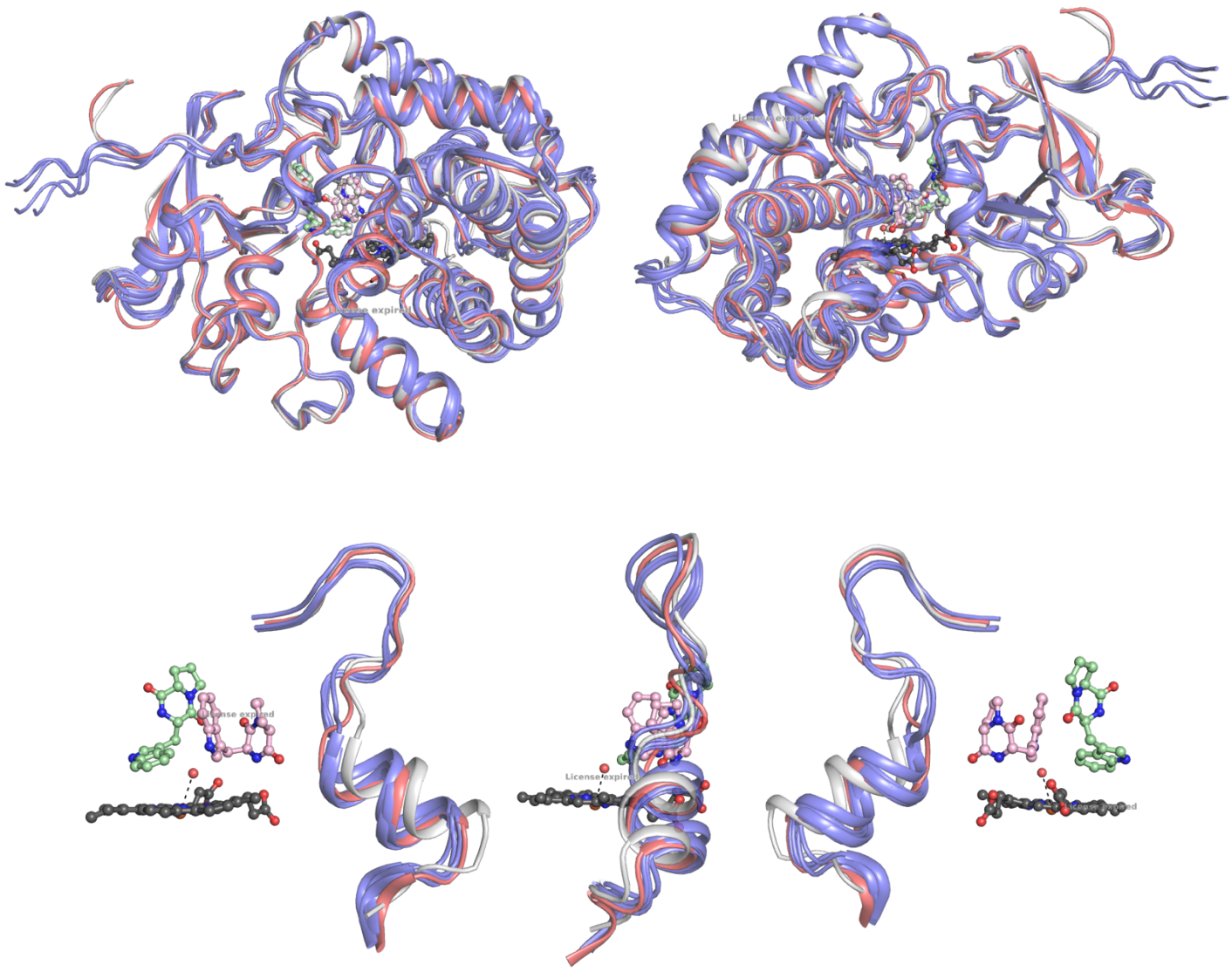

Top: Full size structural overlays of NzeB (grey), AspB (salmon) and top five AlphaFold models (slate blue). Bottom: Zoomed in overlays of NzeB (grey), AspB (salmon) and top five AlphaFold models (slate blue) with residues 80-100 shown which correspond to mobile region identified in molecular dynamics simulations.

References

1. Shende, V.V.; Khatri, Y; Newmister, S.A.; Sanders, J.N.; Lindovska, P.; Yu, F.; Doyon, T.J.; Kim, J.; Houk, K.N.; Movassaghi, M.; Sherman, D.H. Structure and Function of NzeB, a Versatile C-C and C-N Bond-Forming Diketopiperazine Dimerase. *J. Am. Chem. Soc.* **2020**, 142, 41, 17413-17424
2. Battye, T.G.; Kontogiannis, L.; Johnson, O.; Powell, H.R.; Leslie, A.G. iMOSFLM: a new graphical interface for diffraction-image processing with MOSFLM. *Acta crystallographica. Section D, Biological crystallography*, **2011**, 67, 271-281.
3. Winn, M. D.; Ballard, C. C.; Cowtan, K. D.; Dodson, E. J.; Emsley, P.; Evans, P. R.; Keegan, R. M.; Krissinel, E. B.; Leslie, A. G.; McCoy, A.; McNicholas, S. J.; Murshudov, G. N.; Pannu, N. S.; Potterton, E. A.; Powell, H. R.; Read, R. J.; Vagin, A.; Wilson, K. S. Overview of the CCP4 suite and current developments. *Acta Crystallogr D Biol Crystallogr*. **2011**, 67, 235-242.
4. Terwilliger, T. C.; Dimaio, F.; Read, R. J.; Baker, D.; Bunkóczi, G.; Adams, P. D.; Grosse-Kunstleve, R. W.; Afonine, P. V.; & Echols, N. phenix.mr_rosetta: molecular replacement and model rebuilding with Phenix and Rosetta. *Journal of structural and functional genomics*, **2012**, 13, 81–90.
5. Emsley, P.; Cowtan, K. Coot: model-building tools for molecular graphics. *Acta crystallographica. Section D, Biological crystallography*, **2004**, 60, 2126–2132.
6. Adams, P. D.; Afonine, P. V.; Bunkóczi, G.; Chen, V. B.; Davis, I. W.; Echols, N.; Headd, J. J.; Hung, L. W.; Kapral, G. J.; Grosse-Kunstleve, R. W.; McCoy, A. J.; Moriarty, N. W.; Oeffner, R.; Read, R. J.; Richardson, D. C.; Richardson, J. S.; Terwilliger, T. C.; & Zwart, P. H. PHENIX: a comprehensive Python-based system for macromolecular structure solution. *Acta crystallographica. Section D, Biological crystallography*, **2010**, 66, 213–221.
7. Chen, V. B.; Arendall, W. B.; Headd, J. J.; Keedy, D. A.; Immormino, R. M.; Kapral, G. J.; Murray, L. W.; Richardson, J. S.; Richardson, D. C. MolProbity: all-atom structure validation for macromolecular crystallography. *Acta crystallographica. Section D, Biological crystallography*, **2010,** 66, 12–21. https://doi.org/10.1107/S0907444909042073
8. Kabsch, W. XDS. *Acta crystallographica. Section D, Biological crystallography*, **2010**, 66, 125–132.
9. McCoy, A. J.; Grosse-Kunstleve, R. W.; Adams, P. D.; Winn, M. D.; Storoni, L. C.; Read, R. J. Phaser crystallographic software. *Journal of applied crystallography*, **2007**, 40, 658–674.
10. Salomon-Ferrer, R.; Götz, A. W.; Poole, D.; Le Grand, S.; Walker, R. C. Routine Microsecond Molecular Dynamics Simulations with AMBER on GPUs. 2. Explicit Solvent Particle Mesh Ewald. *J. Chem. Theory Comput.* **2013**, 9, 3878–3888.
11. Case, D. A.; Cerutti, D. S.; Cheatham, III, T. E.; Darden, T. A.; Duke, R. E.; Giese, T. J.; Gohlke, H.; Goetz, A. W.; Greene, D.; Homeyer, N.; Izadi, S.; Kovalenko, A.; Lee, T. S.; LeGrand, S.; Li, P.; Lin, C.; Liu, J.; Luchko, T.; Luo, R.; Mermelstein, D.; Merz, K. M.; Monard, G.; Nguyen, H.; Omelyan, I.; Onufriev, A.; Pan, F.; Qi, R.; Roe, D. R.; Roitberg, A.; Sagui, C.; Simmerling, C. L.; Botello-Smith, W. M.; Swails, J.; Walker, R. C.; Wang, J.; Wolf, R. M.; Wu, X.; Xiao, L.; York, D. M.; Kollman, P. A. AMBER 2017, University of California, San Francisco.
12. Wang, J. M.; Wolf, R. M.; Caldwell, J. W.; Kollman, P. A.; Case, D. A. Development and Testing of a General Amber Force Field. *J. Comput. Chem.* **2004**, 25, 1157–1174.
13. Bayly, C. I.; Cieplak, P.; Cornell, W.; Kollman, P. A. A Well-Behaved Electrostatic Potential Based Method Using Charge Restraints for Deriving Atomic Charges: The RESP Model. *J. Phys. Chem.* **1993**, 97, 10269–10280.
14. Besler, B. H.; Merz, K. M.; Kollman, P. A. Atomic Charges Derived from Semiempirical Methods. *J. Comput. Chem.* **1990**, 11, 431–439.
15. Singh, U. C.; Kollman, P. A. An Approach to Computing Electrostatic Charges for Molecules. *J. Comput. Chem.* **1984**, 5, 129–145.

16. Gaussian 09, Revision D.01, Frisch, M. J.; Trucks, G. W.; Schlegel, H. B.; Scuseria, G. E.; Robb, M. A.; Cheeseman, J. R.; Scalmani, G.; Barone, V.; Mennucci, B.; Petersson, G. A.; Nakatsuji, H.; Caricato, M.; Li, X.; Hratchian, H. P.; Izmaylov, A. F.; Bloino, J.; Zheng, G.; Sonnenberg, J. L.; Hada, M.; Ehara, M.; Toyota, K.; Fukuda, R.; Hasegawa, J.; Ishida, M.; Nakajima, T.; Honda, Y.; Kitao, O.; Nakai, H.; Vreven, T.; Montgomery, Jr., J. A.; Peralta, J. E.; Ogliaro, F.; Bearpark, M.; Heyd, J. J.; Brothers, E.; Kudin, K. N.; Staroverov, V. N.; Keith, T.; Kobayashi, R.; Normand, J.; Raghavachari, K.; Rendell, A.; Burant, J. C.; Iyengar, S. S.; Tomasi, J.; Cossi, M.; Rega, N.; Millam, J. M.; Klene, M.; Knox, J. E.; Cross, J. B.; Bakken, V.; Adamo, C.; Jaramillo, J.; Gomperts, R.; Stratmann, R. E.; Yazyev, O.; Austin, A. J.; Cammi, R.; Pomelli, C.; Ochterski, J. W.; Martin, R. L.; Morokuma, K.; Zakrzewski, V. G.; Voth, G. A.; Salvador, P.; Dannenberg, J. J.; Dapprich, S.; Daniels, A. D.; Farkas, O.; Foresman, J. B.; Ortiz, J. V.; Cioslowski, J.; Fox, D. J. Gaussian, Inc., Wallingford CT, 2013.
17. Shahrokh, K.; Orendt, .A; Yost, G. S.; Cheatham III, T. E. Quantum mechanically derived AMBER-compatible heme parameters for various states of the cytochrome P450 catalytic cycle. *J. Comput. Chem.* **2012**, 33, 119–133.
18. Jorgensen, W. L.; Chandrasekhar, J.; Madura, J. D.; Impey, R. W.; Klein, M. L. Comparison of Simple Potential Functions for Simulating Liquid Water. *J. Chem. Phys.* **1983**, 79, 926.
19. Maier, J. A.; Martinez, C.; Kasavajhala, K.; Wickstrom, L.; Hauser, K. E.; Simmerling, C. ff14SB: Improving the Accuracy of Protein Side Chain and Backbone Parameters from ff99SB. *J. Chem. Theory Comput.* **2015**, 11, 3696–3713.
20. Darden, T.; York, D.; Pedersen, L. Particle Mesh Ewald: An N·log(N) Method for Ewald Sums in Large Systems. *J. Chem. Phys.* **1993**, 98, 10089.
21. Shaw, D. E.; Grossman, J. P.; Bank, J. A.; Batson, B.; Butts, J. A.; Chao, J. C.; Deneroff, M. M.; Dror, R. O.; Even, A.; Fenton, C. H.; Forte, A.; Gagliardo, J.; Gill, G.; Greskamp, B.; Ho, C. R.; Ierardi, D. J.; Iserovich, L.; Kuskin, J. S.; Larson, R. H.; Layman, T.; Lee, L.-S.; Lerer, A. K.; Li, C.; Killebrew, D.; Mackenzie, K. M.; Mok, S. Y.-H.; Moraes, M. A.; Mueller, R.; Nociolo, L. J.; Peticolas, J. L.; Quan, T.; Ramot, D.; Salmon, J. K.; Scarpazza, D. P.; Schafer, U. B.; Siddique, N.; Snyder, C. W.; Spengler, J.; Tang, P. T. P.; Theobald, M.; Toma, H.; Towles, B.; Vitale, B.; Wang, S. C.; Young C. Anton 2: Raising the Bar for Performance and Programmability in a Special-Purpose Molecular Dynamics Supercomputer. *IEEE SC* **2014**, 41–53.
22. Sang, R.; Noble, A.; Aggarwal, V. K. Chiral Benzothiophene Synthesis via Enantiospecific Coupling of Benzothiophene S-Oxides with Boronic Esters. *Angew Chem Int Ed* **2021**, *60* (48), 25313–25317.
23. Shaik, S.; Wang, Y.; Chen, H.; Song, J.; Meir, R. Valence Bond Modelling and Density Functional Theory Calculations of Reactivity and Mechanism of Cytochrome P450 Enzymes: Thioether Sulfoxidation. *Faraday Discuss.* **2010**, *145*, 49–70.
24. Park, M. J.; Lee, J.; Suh, Y.; Kim, J.; Nam, W. Reactivities of Mononuclear Non-Heme Iron Intermediates Including Evidence That Iron(III)−Hydroperoxo Species Is a Sluggish Oxidant. *J. Am. Chem. Soc.* **2006**, *128* (8), 2630–2634.
25. Geneste, P.; Olive, J. L.; Ung, S. N.; El Amoudi El Faghi, M.; Easton, J. W.; Beierbeck, H.; Saunders, J. K. Carbon-13 Nuclear Magnetic Resonance Study of Benzo[b]Thiophenes and Benzo[b]Thiophene S-Oxides and S,S-Dioxides. *J. Org. Chem.* **1979**, *44* (16), 2887–2892.